

COPPER REMOVAL FROM REGENERATED PICKLING SOLUTIONS OF
STEEL PLANTS

A THESIS SUBMITTED TO
THE GRADUATE SCHOOL OF NATURAL AND APPLIED SCIENCES
OF
MIDDLE EAST TECHNICAL UNIVERSITY

BY
ESRA SÜTCÜ

IN PARTIAL FULFILLMENT OF THE REQUIREMENTS
FOR
THE DEGREE OF MASTER OF SCIENCE
IN
METALLURGICAL AND MATERIALS ENGINEERING

JANUARY 2020

Approval of the thesis:

**COPPER REMOVAL FROM REGENERATED PICKLING SOLUTIONS
OF STEEL PLANTS**

submitted by **ESRA SÜTCÜ** in partial fulfillment of the requirements for the degree of **Master of Science in Metallurgical and Materials Engineering, Middle East Technical University** by,

Prof. Dr. Halil Kalıpçılar
Dean, Graduate School of **Natural and Applied Sciences** _____

Prof. Dr. Cemil Hakan Gür
Head of the Department, **Met. And Mat. Eng.** _____

Prof. Dr. Abdullah Öztürk
Supervisor, **Met. and Mat. Eng., METU** _____

Assist. Prof. Dr. Metehan Erdoğan
Co-Supervisor, **Metallurgical and Materials Eng. AYBU** _____

Examining Committee Members:

Prof. Dr. Kadri Aydınol
Metallurgical and Materials Eng, METU _____

Prof. Dr. Abdullah Öztürk
Metallurgical and Materials Eng, METU _____

Assist. Prof. Dr. Metehan Erdoğan
Metallurgical and Materials Eng, AYBU _____

Assist. Prof. Dr. Batur Ercan
Metallurgical and Materials Eng, METU _____

Assist. Prof. Dr. Erkan Konca
Metallurgical and Materials Eng, Atılım University _____

Date: 29.01.2020

I hereby declare that all information in this document has been obtained and presented in accordance with academic rules and ethical conduct. I also declare that, as required by these rules and conduct, I have fully cited and referenced all material and results that are not original to this work.

Name, Last name : Esra Sütçü

Signature :

ABSTRACT

COPPER REMOVAL FROM REGENERATED PICKLING SOLUTIONS OF STEEL PLANTS

Sütcü, Esra

Master of Science, Metallurgical and Materials Engineering

Supervisor: Prof. Dr. Abdullah Öztürk

Co-Supervisor: Assist. Prof. Dr. Metehan Erdoğan

January 2020, 87 pages

Pickling is a metal surface treatment technique, made by strong inorganic acids to prepare metals for subsequent processes. The process generates a substantial amount of waste acid because large amount of acid is spent during the process. The impact of the waste acid to the environment is noticeable. The waste solution contains the contaminants of the metal surface and it is also a source of valuable products, metal salts and copper.

When the concentration of copper in the pickling solution exceeds the level of about 100 ppm, randomly plating of copper onto the steel strips which causes visual incompatibility occur. Furthermore, efficiency of pickling decreases with the increase of copper content. Due to their toxic nature, the treatment is mandatory.

The aim of this study is to develop an environmentally-friendly and cost-efficient way for recovery of pickling solution using electrodeposition method. The work consisted of reducing the copper content and to extend the lifetime of the pickling solution by this way. By this process, it was also aimed to reduce the amount of landfilled waste and utilize the needed chemicals.

The work was performed by gathering information from literature but also from industry in Turkey. The work has been a collaboration between the Middle East Technical University (METU), Borcelik and Borusan Technology Department and R&D Co.

Within the scope of copper removal, effects of applied current density, treatable copper concentration and electrolysis duration on copper deposition were studied. Current density was determined as the most effective parameter.

Keywords: Pickling Process, Copper Electrodeposition, Electrochemical Treatment, Current Density

ÖZ

ÇELİK FABRİKALARINDAKİ REJENERE DEKAPAJ ÇÖZELTİSİNDEN BAKIRIN GERİKAZANIMI

Sütçü, Esra
Yüksek Lisans, Metalurji ve Malzeme Mühendisliği
Tez Yöneticisi: Prof. Dr. Abdullah Öztürk
Ortak Tez Yöneticisi: Dr. Öğr. Üy. Metehan Erdoğan

Ocak 2020, 87 sayfa

Dekapaj, metalleri zorunlu şartlar için hazırlayan, inorganik asitlerle yapılan, bir metal yüzey işleme tekniğidir. İşlem önemli ölçüde atık asit oluşturur, çünkü işlem tamamlandığında büyük miktarda asit harcanır. Atık asidin çevreye etkisi belirgindir. Atık çözelti, metal yüzeyin kirleticilerini içerir ve aynı zamanda değerli ürünlerin, metal tuzlarının ve bakırın da kaynağıdır.

Dekapaj çözeltisindeki bakır konsantrasyonu 100 ppm seviyesini aştığında, çelik şeritlerin üzerine rastgele bakır kaplanması meydana gelir ve bu da görsel uyumsuzluğa neden olur. Ayrıca, bakır içeriğinin artması ile dekapaj verimi düşer. Toksik yapıları nedeniyle çözeltinin temizlenmesi zorunludur.

Bu tez çalışmasının amacı, dekapaj çözeltisinin geri kazanımı için çevre dostu ve düşük maliyetli bir elektrokaplama yöntemi geliştirmektir. Çalışma, bakır içeriğinin azaltılmasından ve dekapaj çözeltisinin ömrünün bu şekilde uzatılmasından oluşmaktadır. Bu uygulamayla, atık depolama alanlarındaki atık miktarının azaltılması ve gerekli kimyasalların kullanılması hedeflenmiştir.

Çalışma literatürden ve aynı zamanda Türkiye'deki sanayiden bilgi toplayarak gerçekleştirilmiştir. Çalışma, Orta Doğu Teknik Üniversitesi (ODTÜ), Borçelik ve Borusan Teknoloji Bölümü ile Ar-Ge birimi işbirliğiyle yapılmıştır.

Bakırın uzaklaştırılması kapsamında, uygulanan akım yoğunluğu, işlenebilir bakır konsantrasyonu ve elektroliz süresinin bakır toplama üzerindeki etkileri incelenmiştir. Akım yoğunluğu en etkili parametre olarak belirlenmiştir.

Anahtar Kelimeler: Dekapaj İşlemi, Bakır Elektrokaplama, Elektrokimyasal Muamele, Akım Yoğunluğu

to Samet,

ACKNOWLEDGEMENTS

I would like to express my deepest gratitude to my thesis supervisors, Prof. Dr. Abdullah Öztürk and Assist. Prof. Dr. Metehan Erdoğan, for their helpful guidance, motivation and contributions throughout this study.

I extend my special thanks to the committee members, Prof. Dr. Kadri Aydınol, Assist. Prof. Dr. Batur Ercan and Assist. Prof. Dr. Erkan Konca for their suggestions and comments.

I would like to thank to Borusan Technology Department and R&D Co. for the economical support in the project.

I am thankful to my all labmates Mertcan Başkan, Bengisu Akpınar, Çağlar Polat, Bilgehan Çetinöz, Tansu Altunbaşak, Cemre Yay and Olgun Yılmaz for their supports, Berkay Çağan for his motivation throughout my writing and also Uğurhan Demirci and Oğuzhan Daldal for their technical support. Moreover, special thanks should be given to Büşra Aykaç who encourages me every time. I owe Mustafa Serdal Aras gratitude for sharing his experiences and thoughts.

I especially thank to Pelin Gündoğmuş, Elif Yeşilay, Berk Aytuna, İbrahim Aydın, Seren Özer, Anıl Erdal and Eda Aysal for their friendship.

Moreover, special thanks should be given to Setenay Ünçe, Batuhan Işıklı and Kerem Şengül for their motivation.

I would like to express my gratitude to my parents İshak Karakaya, Ayşe Karakaya.

Lastly, I would like to dedicate this work to my husband Samet Sütçü. Many thanks with all my hearth for the most meaningful support.

TABLE OF CONTENTS

ABSTRACT.....	v
ÖZ.....	vii
ACKNOWLEDGEMENTS.....	x
TABLE OF CONTENTS.....	xi
LIST OF TABLES.....	xv
LIST OF FIGURES.....	xvi
CHAPTERS	
1 INTRODUCTION.....	1
1.1 Production of Secondary Steel.....	1
1.2 Treatment of Steel.....	2
1.3 Treatment of the Spent Pickling Solution.....	3
1.4 Aim of the Study.....	4
2 LITERATURE REVIEW.....	7
2.1 Oxidation of Copper.....	7
2.2 Copper in the Pickling Solution.....	9
2.2.1 Effect of Copper on Regenerated Pickling Solution.....	10
2.3 Copper Removal Techniques.....	11
2.4 Cell Types in Electrochemistry.....	12
2.5 Electrodeposition.....	13
2.5.1 Fundamentals of Electrodeposition.....	14

2.6	Polarization	14
2.7	Hydrogen Evolution.....	16
2.8	Electrodeposition Parameters	17
2.8.1	Current Characteristics	17
2.8.1.1	Direct Current (DC) Method	17
2.8.1.2	Pulse Current (PC) Method.....	18
2.8.1.3	Pulse Reverse Current (PRC) Method.....	19
2.8.2	Physicochemical Parameter	20
2.9	Measurement Techniques	21
2.9.1	Softwares	21
2.9.1.1	Facility for the Analysis of Chemical Thermodynamics (F*A*C*T)	22
2.9.1.2	COMSOL Multiphysics	22
2.9.2	Characterization Techniques	23
2.9.2.1	Inductively Coupled Plasma – Mass Spectrometry (ICP-MS)	23
2.9.2.2	X-Ray Fluorescence (XRF)	24
3	EXPERIMENTAL METHOD	25
3.1	Characteristics of Electrolyte.....	25
3.2	Voltammetric Analysis	26
3.3	Materials	27
3.3.1	Cathode Choice	28
3.3.2	Cathode Preparation	28
3.3.3	Anode Choice	29
3.3.4	Anode Preparation	30
3.4	Experimental Setup.....	30
3.4.1	Laboratory Scale.....	30
3.4.2	Pilot Plant Scale.....	32

3.4.2.1	METU Pilot Plant	32
3.4.2.2	Borçelik Pilot Plant	34
3.5	Copper Removal Measurements	35
3.6	Experimental Design	36
4	RESULTS AND DISCUSSION	39
4.1	Determination of Current Density	39
4.2	Choice of Electrodes	41
4.2.1	Choice of Anode Material	41
4.2.2	Choice of Cathode Material	44
4.3	Choice of Pickling Solution	45
4.4	Effects of Electrolysis Parameters	47
4.4.1	Effect of Initial Copper Concentration on Copper Removal	47
4.4.2	Effect of Current Density and Current Characteristics on Copper Removal	49
4.4.3	Effect of Electrolysis Duration on Copper Removal	50
4.5	COMSOL Multiphysics Analyses	52
4.5.1	Evaluation of METU Pilot Results	56
4.5.2	Evaluation of Borçelik Pilot Plant	61
4.6	Evaluation of Acidity Change during Electrolysis	67
4.7	Energy Consumption	68
5	CONCLUSION	69
	REFERENCES	71
	APPENDICES	
A.	Standard Reduction Potential Table	85
B.	List of Electronegativity Values of Elements	86

C.	Analyzed Elements by ICP-MS.....	87
----	----------------------------------	----

LIST OF TABLES

TABLES

Table 1. Characteristics of regenerated pickling solution.....	26
Table 2. Independent variables and their levels.....	37
Table 3. Full factorial design of experiments	38
Table 4. Table of pilot plant expectations based on laboratory studies	54

LIST OF FIGURES

FIGURES

Figure 1. A Schematic diagram of a pickle line	3
Figure 2. Ellingham diagram for copper and iron oxidations	8
Figure 3. Cell Types (a) galvanic and (b) electrolytic cell	12
Figure 4. Schematic of electrodeposition process	13
Figure 5. The current fluctuation representation for pulse current electrodeposition	18
Figure 6. The current fluctuation representation for pulse reverse current electrodeposition.....	20
Figure 7. Schematic sequence of ICP-MS process.....	23
Figure 8. Schematic view of the voltammetry setup	27
Figure 9. Schematic drawing of experimental setup	31
Figure 10. Schematic view of METU pilot plant from (a) top and (b) side	33
Figure 11. Schematic view of electrode design.....	34
Figure 12. Schematic drawing of pilot plant setup from (a) above and (b) sideways	35
Figure 13. Linear sweep voltammetry of copper containing regenerated pickling solution and corresponding blank solution at a scan rate of 25 mV/s using 1.5 cm ² electrode area.....	40
Figure 14. Change in copper removal for (a) copper and (b) stainless steel cathodes	42
Figure 15. Visual examination of stainless steel cathodes used against (a) titanium, (b) lead and (c) graphite anodes	42
Figure 16. Release of titanium and lead ions for the experiments carried out with Titanium and Lead anodes using (a) copper and (b) stainless steel cathodes	43
Figure 17. Comparison of copper removal of regenerated and spent pickling solution	46

Figure 18. Main effect of initial copper concentration of the regenerated pickling solution on copper removal.....	48
Figure 19. Main effect of current density on copper removal by (a) direct current method and (b) pulse current method for copper and stainless steel cathodes	49
Figure 20. Main effect of electrolysis duration on copper removal by (a) direct current and (b) pulse current method for copper and stainless steel cathodes.....	51
Figure 21. The results of COMSOL multiphysics solution of designed pilot plant showing total electrode thickness change after 6-hours of electrolysis.....	52
Figure 22. Change in copper content with time for a current density of 100 A/m ² with plate copper and stainless steel cathodes	57
Figure 23. Comparison of current method with respect to electrolysis duration for s-shape stainless steel cathodes at 130 A/m ² current density	58
Figure 24. Comparison of cathode shape with respect to electrolysis duration at 130 A/m ² current density	59
Figure 25. Comparison of effect of current density on stainless steel plate cathode	60
Figure 26. Borçelik pilot test at 100 A/m ² pulse current density.....	62
Figure 27. Borçelik pilot test at 130 A/m ² pulse current density.....	63
Figure 28. Borçelik pilot test result from 127 ppm initial copper concentration performed at 130 A/m ² pulse current density	64
Figure 29. Copper plated stainless steel cathode	64
Figure 30. Borçelik pilot test at 150 A/m ² direct current density	65
Figure 31. Borçelik pilot test for 24-hours of electrolysis at 150 A/m ² direct current density	66
Figure 32. Change in conductivity with respect to electrolysis duration.....	67

CHAPTER 1

INTRODUCTION

1.1 Production of Secondary Steel

Steel is one of the most recycled materials in the world. The recovery rate of the steel is about 90% [1]. Therefore in most steel plants, the main raw material of steel is the scrap steel [2]. As a result, the secondary steel industry is growing all over the world [3].

During the production of secondary steel, firstly raw materials are melted in the electrical arc furnaces. During melting, the temperature of the arc and molten steel rises to 3500 and 1800°C, respectively. Then carbon, sulfur, and nitrogen in the molten mixture are removed by a steel converter [2].

The steel scrap contains alloying elements and undesired metals which should be transferred to the slag [1]. Undesired metals are needed to be extracted in the electrical arc furnaces' slag. These metals are called 'tramp elements'. Other than the alloying elements, according to thermodynamic analysis, the most important tramp elements in the recycling of steel are copper and tin [4].

For a qualified steel production, the liquid steel is sent to the ladle station to get rid of unwanted materials and to homogenize both the temperature and chemical composition. After the ladle station, the liquid steel is cast in the continuous casting machine or in the ingot casting area. By the cooling process; the steel solidifies in the cast [2].

Currently, copper cannot be removed from steel in commercial processes [3]. The source of the copper in the scrap is mostly copper wires and automobile motors [5].

Turkey is the world's ninth-largest steel exporter and exports steel to more than 200 countries [6]. Its steel production relies heavily on scrap which makes the Turkish steel contain some amount of copper [7].

1.2 Treatment of Steel

The surface of the steel should be clean, smooth and flawless because of its purpose of use and its corrosion resistance [8].

During manufacturing operations of steel, the corrosion resistance of the material may decrease. Thus, a surface cleaning process is required to restore the quality [9]. There are chemical and mechanical cleaning methods for manufactured steel. Superior results are expected from chemical treatments because of their ability to reduce surface contamination risk [8].

The chemical treatment for the surface cleaning of a stainless steel manufacturing includes electropolishing and pickling for the removal of oxide, iron and inorganic contaminations without creating any damage on the surface.

Pickling is the most common chemical metal surface treatment technique. It is used to get rid of oxides, stains, rust, scale, inorganic contaminants, and/or other impurities that are coming from metals and alloys [8]. The pickling solution aims to react with the oxides and/or other impurities together with the base metal and to give metal salts as product [10]. Aggressive inorganic acid, such as sulphuric acid (H_2SO_4), hydrochloric acid (HCl), the mixture of nitric acid (HNO_3) and hydrofluoric acid (HF) are used in the pickling process [11].

Pickling process can be applied in the way of immersing the metallic materials, especially steel coils, into a pickling bath and make it pass through the pickling solution [12]. In ordinary steel plants, pickle lines consist of four pickling tanks, which are filled with pickling solutions. The pickling process starts from one end of the line through the other end and the pickling solution counter flows according to the strip as shown in Figure 1. Therefore, the acid concentration and the efficiency

of the pickling tanks diminishes from the starting point of the pickling process to the endpoint [13].

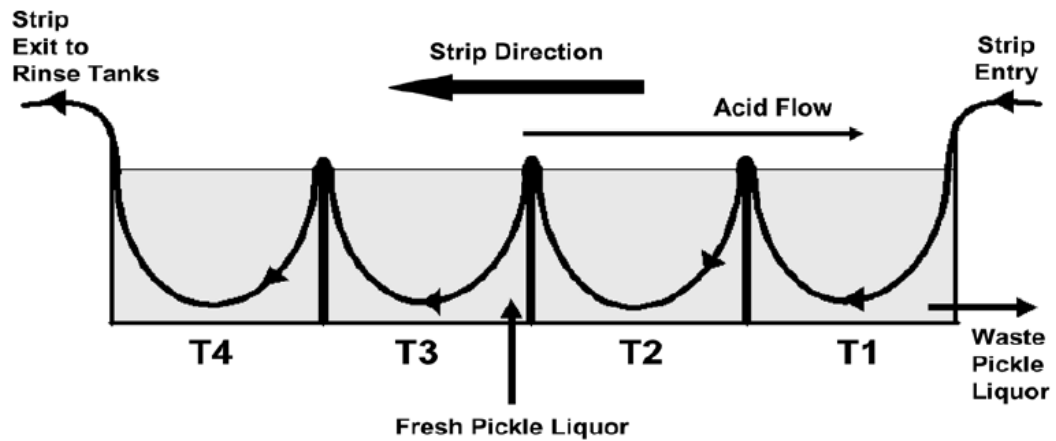


Figure 1. A Schematic diagram of a pickle line

1.3 Treatment of the Spent Pickling Solution

The efficiency of the pickling solution depends on the acid concentration, temperature and free metal content of the bath [14]. When the pickling process is done, the acid produces dissolved metal salts and after several processes, acid neutralization occurs [8, 10]. The produced metals from the process depend on what the treated metal object is [15]. When the concentration of acid decreases and the free metal content of the bath increases, the acid becomes spent [16].

During the pickling process, a large amount of acid is spent [10] due to the chemical reactions between the solution and the surface scales of the metal [17]. The spent pickling solution contains valuable metals, metal salts and acid [18] such as iron, chromium, lead, copper, nickel, and zinc together with the residual free acid or any other metals depending on the pickled material [10]. Due to containing high concentration of heavy metals and presence of strong acid, the spent pickling

solution is classified as a hazardous material [19]. The strong regulations of acid and metal disposal and environmental and economic aspects force steel plants to regenerate the effluents and reuse them [20].

Regeneration is the recovery of waste pickling solution. It is a way of treatment of strong acid and extraction of ferric oxide [21]. Pickling acid (HCl) consumes when the iron chloride content of the solution is saturated. Both spent pickling solution and iron chloride can be recovered by thermal decomposition of the solution into gaseous HCl and iron oxide. In the regeneration process, iron chloride containing spent pickling acid is sprayed directly into a heated reactor and fine powdered iron oxide and gaseous form of HCl are formed [22, 23]. Recovery of the hydrochloric acid solution by the regeneration process is cheap and provides iron oxide for future uses. Waste gases from thermal decomposition are cleaned by rinsing water and this reduces the pollution of waste gases [22].

At the end of the regeneration process, only some amount of copper in the solution can be oxidized. Increased copper concentration in the pickling solution causes deposition of copper on the metal in the following pickling processes [13]. Therefore, despite the regeneration process, it is necessary to destroy the acid.

1.4 Aim of the Study

The aim of this study is to make an evaluation for preventing the copper deposition problem of the pickling solution by keeping the copper level of regenerated pickling solution below 100 ppm and to extend the lifetime of the pickling solution by developing an environmentally-friendly method of electrodeposition. By this process, it is also aimed to reduce the amount of landfilled wastes.

In order to design a process in this context, laboratory scale studies were carried out to determine the optimum current density, electrolysis duration and treatable copper concentration of the pickling solution by taking into consideration the amount of removed copper. Originated from the laboratory scale data, pilot scale applications

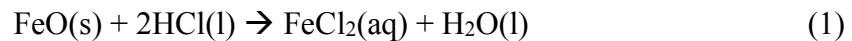
were performed to test the scale-up potential of the process, which produced promising results at laboratory scale.

CHAPTER 2

LITERATURE REVIEW

2.1 Oxidation of Copper

The spent pickling solution can no longer be used when it reaches saturation. The saturated solution is filled with iron chloride. The iron chloride formation is shown in equation (1)



The spent HCl solution and iron chloride is decomposed into iron oxide and gaseous HCl with the help of regeneration process as shown in equation (2). The regenerated HCl is then condensed and fed to the pickling line to be reused [22].



The regeneration process only delays the disposal time of the solution because the process removes the solution from impurities but copper ions are still present in the solution [13].

From the Ellingham diagram, it is possible to obtain the equilibrium data of a metal and its oxide. The diagram is plotted as standard Gibbs Energy of formation (ΔG°) for the oxidation reactions based on consumption of 1 mole of O_2 versus temperature. The slopes of the lines give the standard entropy change. The curves follow a linear line as long as there is no phase change [24].

The Ellingham Diagram for copper and iron oxidations are given in Figure 2. The equation (3) shows the copper oxide formation reaction. Ellingham Diagram shows the stability of oxide forms of copper and iron as a function of temperature. Due to the diagram, the lines closer to the top (Copper) are more noble and their oxides are

unstable and more easily reduced. From top to bottom of the diagram, metals are more reactive, unstable and it is harder to reduce the oxides [24, 25].



As can be seen in Figure 2, oxide forms of copper are above oxide forms of iron in the corresponding Ellingham Diagram. Therefore, once in steel, it is not possible to get rid of copper by oxidizing and sending to the slag phase because iron will get oxidized before the required oxygen partial pressure for copper oxidation is achieved.

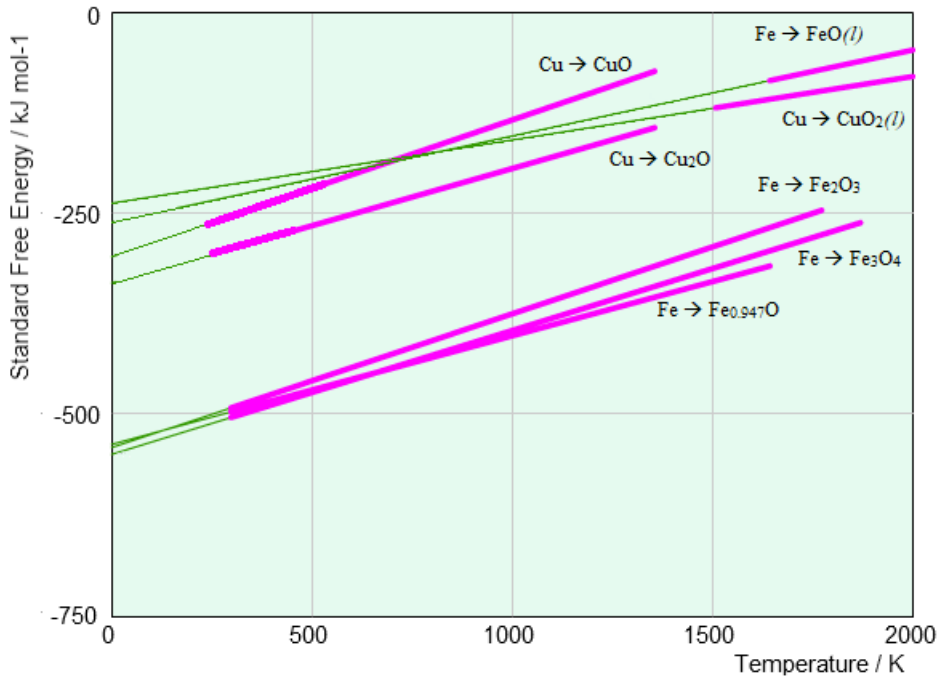
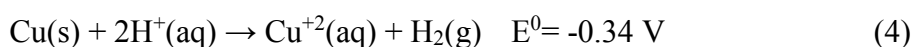


Figure 2. Ellingham diagram for copper and iron oxidations

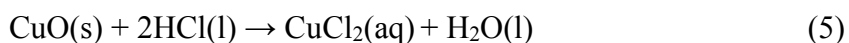
2.2 Copper in the Pickling Solution

The reaction between a metal and an acid is called a redox reaction. But copper metal has low interaction capacity to react with HCl. Therefore, it does not react with HCl acid under normal circumstances because its reduction potential is higher than the reduction potential of hydrogen. Reaction (4) shows the activity series of copper and hydrogen, and their calculated potentials [26]. All of the reduction potentials are given in Appendix A.



The negative potential shows that copper cannot react with non-oxidizing acids such as HCl. But as any other metals, oxidation of copper is possible. The oxidation reaction takes place when the copper is exposed to air. There is no oxygen radical exist in HCl to react with copper but a dilute HCl acid dissolves some amount of air in it to form copper oxide. Reaction (3) shows the transformation of copper into copper oxide.

Copper (II) oxide does react with HCl acid. Since metal oxides are basic substances, reaction between copper (II) oxide and HCl acid results in formation of respective salt and water which is non-redox but a neutralization reaction [27]. Reaction (5) shows the transformation of copper (II) oxide into copper (II) chloride.



When the oxidized copper is exposed to hydrochloric acid solution, a double replacement reaction takes place and copper (II) oxide dissolves in the acid to form copper (II) chloride solution [28].

ICP-MS analysis is the trustable way for the determination of copper ion concentration of the solution. By this way, particles can be converted into first atoms, then into ions by ICP source, and MS source determines the mass of the selected ions [29]. Therefore, the technique measures the mass of the selected cation; copper [28].

2.2.1 Effect of Copper on Regenerated Pickling Solution

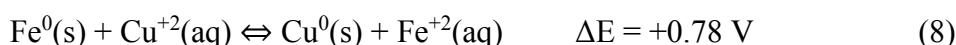
Cementation is one of an important hydrometallurgical unit process [30]. It is the extraction of a more noble metal from the electrowinning or electroplating solution and precipitation onto a more electropositive or less noble metal. All of the electronegativity values are given in Appendix B.

One of the most popular and spontaneous example of cementation is the precipitation of copper on iron [30]. In the copper cementation reaction, exchange of electrons between the dissolving iron and precipitating copper occurs. At the end of the reaction, copper cements onto the surface of the iron [31].

There are two redox half reactions in the cementation process. One of them is the spontaneous reduction of copper, contained in an electrolyte, which is more noble than iron, and the other one is the oxidation of iron as given in equations (6) and (7) [32].



The global cementation reaction of copper ions by iron is given in equation (8) where the total cell potential is positive which makes the reaction spontaneous [33].



The strongest influential factor on copper cementation is initial copper ion concentration of the solution [34]. When the copper ion concentration in the regenerated pickling solution increases and exceeds the level of about 100 ppm, the solution results in copper cementation problem onto the steel strip randomly with varying severity in the following pickling processes [13].

Influence of temperature of the solution is non-negligible. Increasing temperature has a positive effect on the cementation due to the decreasing viscosity and

increasing bulk diffusivity of copper ions together with the mass transfer coefficient [34].

2.3 Copper Removal Techniques

Heavy metal contamination has turned out to be a standout amongst the most genuine ecological issues today. The problem is, heavy metals and heavy metal containing fluids are not biodegradable and they have tendency to aggregate in living organisms and most of them known as poisonous or carcinogenic which is accepted to be a risk for human beings and other living cells [35].

Copper is one of the harmful heavy metal concern in treatment of industrial effluents. Directly or indirectly discharging of copper containing fluid is widely encountered. The treatment of the metal is of exceptional worry because of its unmanageability, recalcitrance and persistence in the environment [36].

There are several treatment methods developed for metal recovery operations. These methods include; chemical precipitation [37–41], ion exchange [41–44], solvent extraction [45–50], membrane technology [15, 50, 51], acid swapping and cementation [52], adsorption [50,53] and electrochemical treatment [54–58]. For a cost-effective and environmental solution, electrodeposition method is a promising technique for recovery of some metals from waste solutions using insoluble anodes [52].

Electrodeposition is defined as the process of depositing a material onto a conducting surface from a solution containing ions by passing a current through an electrochemical cell from an external source [59]. The process is advantageous due to its low cost, industrial scale and complex shape applicability and cleanliness [60].

2.4 Cell Types in Electrochemistry

There are two types of electrochemical cells that follow faradaic current; galvanic (voltaic) cell and electrolytic cells. A voltaic cell is a device that converts chemical energy into electrical energy. The cell uses the energy, that is released from a spontaneous redox reaction where Gibbs free energy change of the system is negative, to produce electrical energy. The schematic view of the voltaic cell is shown in Figure 3 (a). On the other hand, an electrolytic cell is a device that converts electrical energy into chemical energy. The cell uses the electrical energy, which is produced from an external source to produce a nonspontaneous redox reaction where Gibbs free energy change of the system is positive. The schematic view of the electrolytic cell is shown in Figure 3 (b). A cell used in electrodeposition is a kind of electrolytic cell.

As a common feature, both of the cells have two conducting electrodes, one of them is anode where oxidation reaction takes place and the other one is cathode where reduction reaction takes place and the electron flow is from anode through cathode [61].

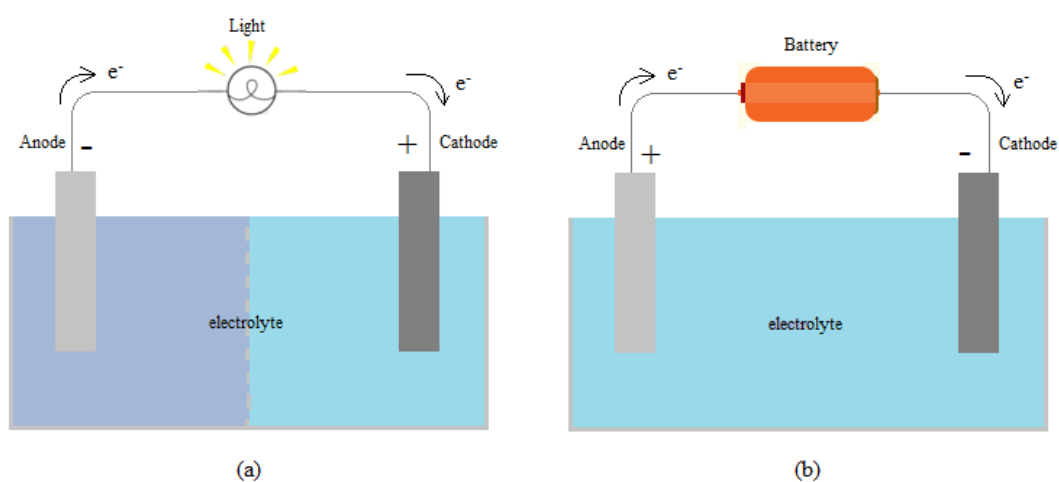


Figure 3. Cell Types (a) galvanic and (b) electrolytic cell

2.5 Electrodeposition

Electrodeposition is an electrolysis process that leads to deposition of a metal or an alloy onto a conducting surface in an aqueous medium. The deposited metal depends on the conducting surfaces and/or chemistry of the solution [59].

An electrolysis cell consists of conducting surfaces; anode and cathode, an electrolyte and a power supply that generates current. Anode is the positive electrode, which can be made up of either soluble or inert material, where oxidation reaction takes place, and cathode is the negative electrode, where reduction reaction takes place and electrodeposition occurs by the help of applied external current on the system [62].

The mechanism of the process is by means of reduction of a metal cation (M^+), to prepare a metallic or metal-alloy film (M) on the cathode electrode [63]. The schematic of electrodeposition process is shown in Figure 4. In the process, firstly, positively charged particles form in the aqueous solution. Then, these particles are transferred from bulk through the cathode surface by means of a mass transfer mechanism. Finally, electrodes and particles interact and particles merge with growing metal layers and irreversible entrapment occurs [64].

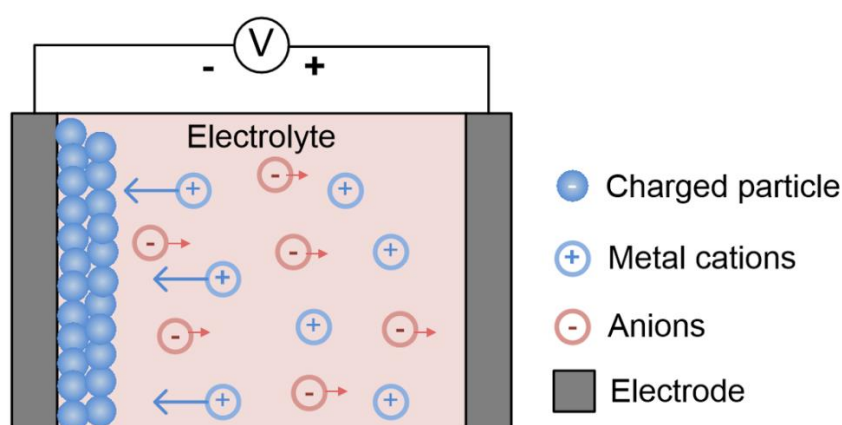


Figure 4. Schematic of electrodeposition process

A general purpose of the electrolysis process is to recover metals from aqueous solutions. It is also an economical and flexible method that can be applied on complex shapes to produce a coating [65]. It is a multifaceted, valuable and clean process and can be scaled up to industrial applications. Furthermore, the deposited metal is pure and the amount can be controlled in the process by monitoring the charge passed through the system [66].

2.5.1 Fundamentals of Electrodeposition

The theory of electrodeposition is based on the Faraday's law. Faraday's law gives the quantitative amount of deposit, in grams (W), at the cathode (Eq. (9)) in the form of relation between the total charge passing from the cell (Q_c) (Eq.(10)) in coulombs and the electrochemical equivalent of the metal (z_c) (Eq.(11)).

$$W = \eta_{eff} \times \int M I \partial t / nF \quad (9)$$

$$Q_c = \int I \partial t \quad (10)$$

$$z_c = M / nF \quad (11)$$

where I is the current applied on the system in amperes, t is the application time in seconds, M is the molecular weight of the depositing metal, n is the number of reducing electrons, F is the Faraday constant that is 96,485.0 coulombs (amp-sec) and η_{eff} is the current efficiency [61].

2.6 Polarization

In an electrochemical reaction, the Gibbs free energy change of the reaction must be equal to the electrical energy produced by the system for a reversible case. The equality case is not possible when the external electromotive force is larger than the

capacity of the system. Equation (12) gives the minimum energy needed to operate the system in joules [67].

$$W = zFE_{cell}^0 \quad (12)$$

where zF is the electrical charge in coulombs and E_{cell}^0 is the formal potential in volts [68].

The operating cell potential (E_{cell}) can be described with the help of Nernst equation as shown in equation (13) [67].

$$E_{cell} = E_{cell}^0 + \frac{RT}{zF} \ln \frac{M_O^*}{M_R^*} + C \quad (13)$$

The potential is in the form of sum of the standard potential, the concentration term and polarization factor; where E_{cell}^0 is the formal potential (V), R is the gas constant (8.314 J/mole.K), T is the absolute temperature (K), z is the number of electrons transferred, F is the Faraday constant, M_O^* and M_R^* are bulk concentrations and C is the polarization factor in the electrodeposition process.

For an irreversible case, the operating cell potential (E) is significantly different from the equilibrium potential (E_{eq}). The extent of this new potential is known as overpotential (η) in volts and the situation is termed as polarization. The overpotential calculation is shown in equation (14) [69].

$$\eta = E - E_{eq} \quad (14)$$

The overpotential value is more negative for cathode and more positive for anode overpotentials due to the increase in current density. The relation between current and overpotential is exponential as represented in equation (15) and obeys Tafel equation [70].

$$\eta = a + b \log i \quad (15)$$

where a and b are constants bound up with current density, solution composition, electrode material and temperature [67].

The basic polarizations are concentration polarization (η_{conc}) and activation polarization (η_{act}). The concentration polarization at the electrode surface depends on the reactant consumption therefore the polarization is affected by the activity of the ions at the electrode surface and bulk. It is possible to see the concentration polarization in the case of hydrogen evolution due to the change in hydrogen concentration at the electrode surface, which can also be named as ‘hydrogen polarization’. In the case of polarization, it may also be important to overcome the activation energy barrier of a reaction. This type of polarization is the activation polarization. [58, 71].

To overcome the overpotential, the amount of current that must be applied on the system is the summation of anodic and cathodic current densities that is shown in the Butler-Volmer Equation as shown in equation (16).

$$i = i_0 \left\{ \exp \left[\frac{\alpha_a n F \eta}{RT} \right] - \exp \left[- \frac{\alpha_c n F \eta}{RT} \right] \right\} \quad (16)$$

where i is the current density, i_0 is the exchange current density, n is the number of transferred electrons, α_a is the anodic transfer coefficient and α_c is the cathodic transfer coefficient, F is the Faraday constant, η is the overpotential and R is the gas constant [72].

2.7 Hydrogen Evolution

During the electrodeposition process, hydrogen evolution reaction (HER) takes place on the cathode beside the deposition reaction. Therefore the hydrogen evolution causes inefficiency during the process [73]. Equation (17) shows the discharge of hydrogen in the acidic solution at the cathode [74]. Hydrogen is absorbed as H^+ atoms by the cathode, but the atoms combine and H_2 molecules are formed. Hydrogen is desorbed from the cathode surface and diffuses from the electrolyte in gaseous form [75].



The higher the current density, the more the hydrogen evolution on the cathode [76].

2.8 Electrodeposition Parameters

2.8.1 Current Characteristics

Current density is one of the most important parameters in electrodeposition process due to its impact upon the cost, deposition composition and mechanical properties of the coating [65].

Metal deposition rate increases with increasing current density, but the increase is logarithmic due to the undesired side reactions [17]. When the variables that affect the current efficiency are compared, the effect of current density on current efficiency is one of the most significant factors [77].

A process can be carried out by using direct, pulse and pulse reverse current methods [65]. The aim of using different techniques is to enhance the incorporation and to consolidate the deposition [64].

2.8.1.1 Direct Current (DC) Method

Direct current method is the oldest and conventional electrodeposition process technique. The current is continuously applied on the system without any interruption. The method is more simple and economic, and the technology that is needed to apply DC is easier to find [65].

2.8.1.2 Pulse Current (PC) Method

Pulse current method increases the mechanical properties, incorporation and homogeneity when compared to DC method. The method controls the microstructure, chemical composition and deposition morphology.

In the PC electrodeposition the current follows a periodic manner that moves between a current and a zero current [65]. The current fluctuation with time representation is shown in Figure 5.

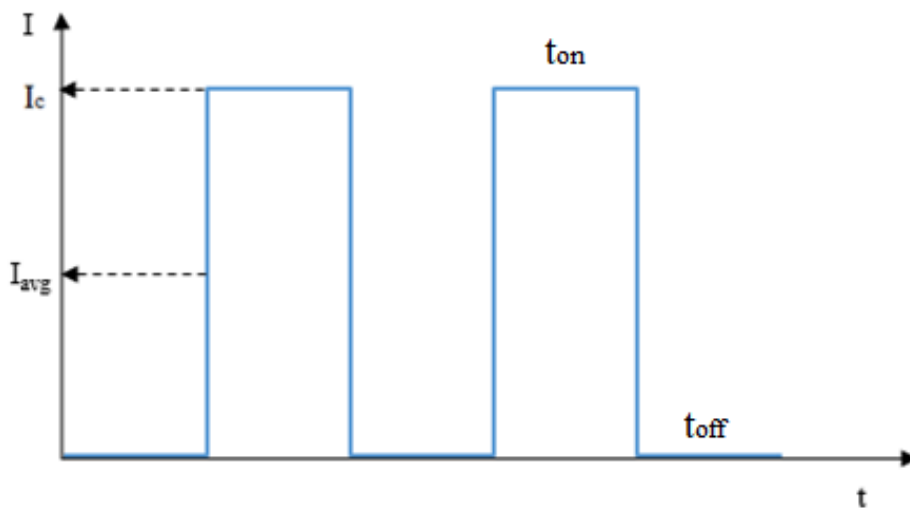


Figure 5. The current fluctuation representation for pulse current electrodeposition

PC method depends on; on time (t_{on}) and off time (t_{off}) for pulse and the cathodic current (I_c). The parameters determine the composition, thickness and morphology of the deposit. By this technique, it is possible to increase the number of grains and create finer grain sized deposition [78]. The average current (I_{avg}) that is applied on system can be calculated by using equation (18) [64].

$$I_{avg} = \frac{I_c \times t_{on} + (0) \times t_{off}}{t_{on} + t_{off}} \quad (18)$$

2.8.1.3 Pulse Reverse Current (PRC) Method

Pulse reverse current method ensures uniform deposition, and empowers the particle incorporation. The method has the advantage to deposit lower concentrated ions with the result of satisfactory chemical composition and morphology. The method helps lower the internal stress with respect to DC method. It is better to use the technique for composite coatings [64].

The current efficiency of PRC method is not as much as the PC method. The parameters of PRC method are time of pulse (t_{on}), off time (t_{off}), reverse time (t_{rev}), height of peak (I_c), height of the reverse peak (I_a) and average current (I_{avg}). The average current calculation is as shown in equation (19).

$$I_{avg} = \frac{I_c \times t_{on} - I_a \times t_{rev}}{t_{on} + t_{rev} + t_{off}} \quad (19)$$

where I_a is the anodic current, I_c is the cathodic current, t_{on} is the cathodic (forward) time, t_{rev} is the anodic (reverse) time [78]. The current fluctuation with time representation is shown in Figure 6.

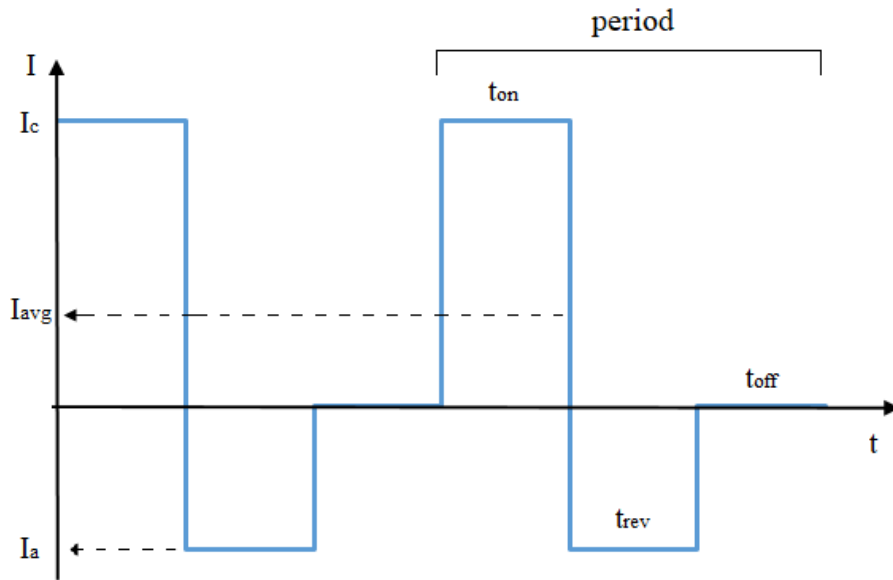


Figure 6. The current fluctuation representation for pulse reverse current electrodeposition

2.8.2 Physicochemical Parameter

Structural and optical properties and quality of the deposit depend on the physicochemical characteristics of the solution, such as conductivity, ion concentration, pH and temperature. Therefore these are important parameters for electrodeposition [79].

The quality of the deposition increases with increasing conductivity [79] and arranging pH of the solution. These parameters affect the crystal and physical structure of the coating [80].

Conductivity of solutions depends on the concentration of the solution. In other words, higher concentration triggers the conductivity of electrolyte. The characteristics of coatings are better when high conductive solutions are used because conductivity is one of the main factor that effects the throwing power together with the plating ability of the solution to produce a uniform coating [81].

Ion concentration is another significant parameter for electrodeposition because the deposition amount depends on the amount of ions that come through the cathode [77]. Therefore, when the ion concentration increases, the amount of deposition increases [82]. At the same time, when insoluble anodes are used, the ion concentration in the electrolyte decreases when the ions reach the cathode surface so the amount and rate of deposition decreases [83].

Number of positively charged particles run counter to the pH value, furthermore, low pH value causes a decrease in current efficiency. There is some evidence that the current efficiency of the coating and content of depositing material decreases with decrease in pH value [80]. The decrease in pH results in a sharp decrease in amount of deposition [82]. pH of the solution has great effects on the composition, growth mechanism, grain orientation, microstructure, morphology and surface quality of the deposit [80, 84, 85].

Temperature is a well-controlled and significant factor for electrodeposition. The parameter has effects on both physical and mechanical properties [80, 86] and quality of the deposit [79]. The effect of electrolyte temperature on the amount of deposit differs with respect to the combination of electrolyte and the particles that deposit [87].

There is some evidence that the deposition amount and current efficiency can increase [88], decrease [89] or remain constant [90] with increasing temperature [87].

2.9 Measurement Techniques

2.9.1 Softwares

Different software programs are available for the chemical equilibrium determination, modelling, and simulations. Here, F*A*C*T and COMSOL Multiphysics softwares are explained briefly.

2.9.1.1 Facility for the Analysis of Chemical Thermodynamics (F*A*C*T)

F*A*C*T (Facility for the Analysis of Chemical Thermodynamics) is an online database developed for thermochemical analysis and thermodynamic calculations. It is initially created for chemical metallurgists and now it is used in the field of chemical engineering, corrosion engineering, organic chemistry, geochemistry, ceramics, electrochemistry, etc. The software enables researchers and engineers to analyze chemical reactions with its reliable database [91].

2.9.1.2 COMSOL Multiphysics

COMSOL Multiphysics is a fast and efficient finite element modelling software that involves every step of the workflow, starting from defining geometry to physics in order to solve the problem and achieve trustable results, of a model [92]. It is possible to simulate the experiments and prototypes, which is composed of more than one physics phenomena, by making design and process optimizations with this software. The software is designed to be utilized by engineers, scientists and researchers [93]. It is used in all fields of engineering, manufacturing and researches to simulate designs, devices and processes [92].

It is possible to draw 1, 2 and 3D solid structures and/or import CAD and ECAD files, make changes on them and repair by using the software. In order to model extensive variety of physics phenomena, the software has predefined physics interfaces [93].

The aim of using the software is to attempt hypothetical work without needing master learning of numerical analysis [92].

2.9.2 Characterization Techniques

2.9.2.1 Inductively Coupled Plasma – Mass Spectrometry (ICP-MS)

ICP-MS (Inductively Coupled Plasma - Mass Spectrometry) is a sensitive analytical technique that is a rapid way of trace element determination. The system can detect almost all elements, comprising certain non-metals, many of halogens, alkali and alkaline earth elements, rare earth elements, transition metals and other metals and metalloids, with high scanning speed. It has wide analytical range of measurements up to ppt levels and it is possible to obtain isotopic information and make multi-element characteristics by using the system.

The utilization areas of the system include environmental, geochemical, semiconductor, clinical, nuclear, chemical, and metallurgical applications.

The system combines inductively coupled plasma with a mass spectrometer. This serves the user to convert elements firstly into atoms and then into ions by ICP source, and to separate and detect the mass of the ions by MS source. The sequence of the process of the device is given in Figure 7.

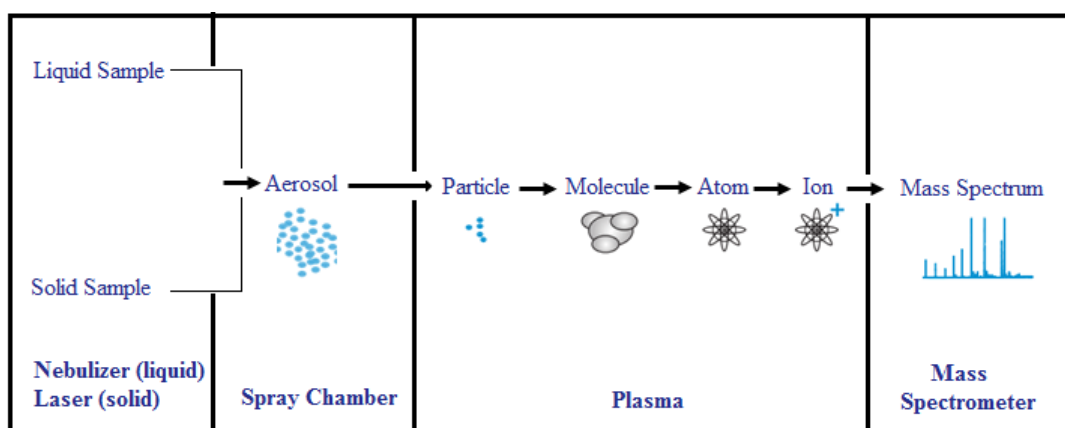


Figure 7. Schematic sequence of ICP-MS process

The system consists of different parts:

- Sample introduction part: Sample is introduced to ICP in aerosol form.
- Ion generation part: Aerosol sample passed into plasma, which is made up of argon stream, and dried, decomposed, vaporised and atomized then ionized by the removal of one electron from each atom with the effect of high temperature of the plasma.
- Plasma/vacuum interface part: Positively charged ions are extracted in.
- Ion focussing part: The ions passed through the MS and photons and residual neutral material separation of ions occurs.
- Ion separation and measurement part: Each ion is detected and total mass is stored.

The result of the ICP-MS analysis is given by a spectrum. The detected spectrum on periodic table is given in Appendix C. The size of each peak of the spectrum is directly proportional to the concentration of the element in the sample [29, 94].

2.9.2.2 X-Ray Fluorescence (XRF)

XRF is an analytical measurement device that does not have any destructive effects during the tests and it is used to make elemental detection of a sample even if it is solid, liquid, slurry or a powder form [95, 96]. It is also possible for the device to measure the thickness of coatings [96].

The working principle of the device is that any type of sample absorbs the X-ray fluorescent and the X-ray excites the energy level from 1 to 2 and the device measures the emitted fluorescent, while the energy state is dropping from 2 to 1, to analyze the quality and quantity of the elemental composition of the sample. The emitted fluorescents produce characteristic X-rays that is unique for every element [95]. The device can analyze wide variety of elements in ranges from weight percent to sub-ppm levels [96].

CHAPTER 3

EXPERIMENTAL METHOD

The laboratory scale applications were performed to determine the optimum current density, electrolysis duration and treatable copper concentration of pickling solution by taking into consideration the amount of removed copper.

3.1 Characteristics of Electrolyte

During the copper electrowinning from dilute solutions, the deposition morphology differs in the presence of other metals [97]. Electrolytic copper extraction is less effective when the amount of non-ferrous metal ions are higher in the solution [98]. Studies also showed that in the presence of iron, the deposited product consists of metal oxides and hydroxides [17] and current efficiency during the copper electrowinning decreases proportionally with the ferric ion concentration in the solution [99, 100]. Therefore, regenerated pickling solution was used in this study instead of spent pickling solution.

Regenerated pickling acid solution was collected from Borçelik steel plant located in Bursa, Türkiye. The non-used pickling solution was composed of pure HCl solution (37% HCl) and the regenerated pickling solution contained trace amounts of copper and iron ions.

The characteristics of the effluent were determined by pH, conductivity and acidity measurements. The characteristics are given in Table 1.

Table 1. Characteristics of regenerated pickling solution

Characteristics of Effluent	<i>Content</i>
pH	-0.5
Conductivity (mS/cm)	~800
Acidity (g/L)	185
Color	Yellow
Odor	Purgent. Irritating (Strong)

For the characterization of the regenerated pickling solution, Thermo Scientific Orion Star A215 Benchtop meter kit was used for both pH and conductivity measurements.

3.2 Voltammetric Analysis

Before starting the systematic experiments, voltammetric analysis were performed to determine the current density range and avoid side reactions for copper electrodeposition from regenerated pickling solution of steel plants. Linear sweep analysis showed that more negative potentials resulted in too much hydrogen evolution at the cathode and chlorine evolution at the anode in a previous study [101]. The side reactions affect the current efficiency of the system. Therefore, in order to abstain from side reactions and enable copper reduction, optimum operating voltage values for the electrochemical cell should be found.

The range of applied current density was determined by linear sweep voltammetry (LSV). LSV was performed using a two-electrode setup by Gamry Instruments Reference 3000. The working electrode was a copper foil and a graphite rod was used as the counter and the reference electrode. The schematic view of voltammetric cell is shown in Figure 8. The voltammetric response of electrodeposition of copper between the anode and cathode in the regenerated pickling solution was recorded during the analysis. The voltammograms were obtained from ‘Echem Analyst’ program.

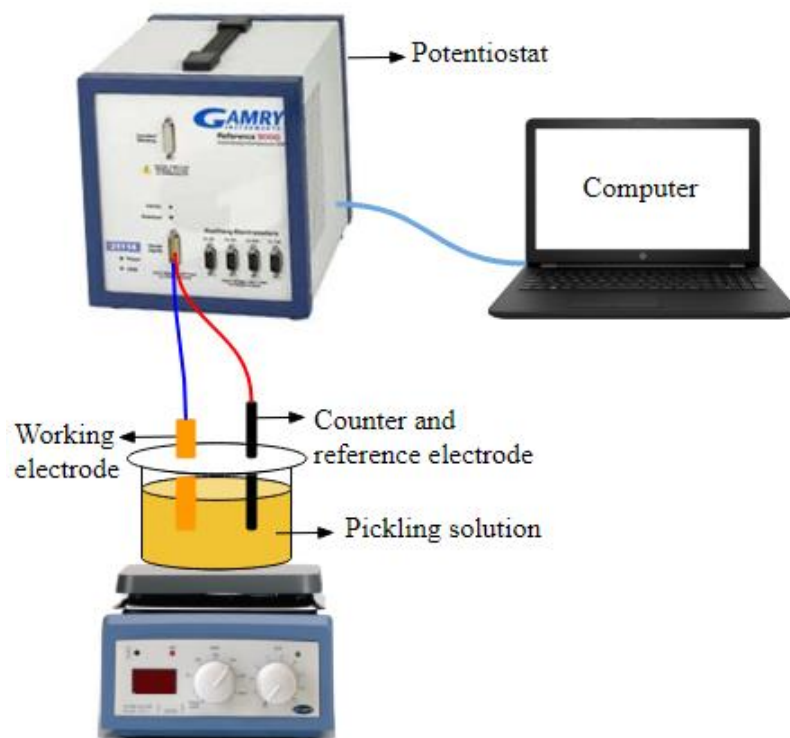


Figure 8. Schematic view of the voltammetry setup

3.3 Materials

A set of preliminary experiments were performed to select promising anode and cathode materials to be tested in systematic experiments. During the selection of electrode materials, ICP-MS analyses of the solution, precision scale measurements and XRF analyses of the deposits were evaluated.

For the characterization of the pickling solution, Agilent 7700x ICP-MS equipment was used for ICP-MS analysis. To determine the removed and therefore collected copper amount, ICP-MS analysis was done on the pickling solution before and after the electrolysis experiments.

Precision scale (Precisa 152A) measurements and XRF (Fischerscope X-Ray XDV-SDD 604-447) analysis were done on the cathode to determine the collected copper amount.

When the amount of collected copper, deposit composition and deposit morphology were taken into consideration, copper and 304 stainless steel were selected as cathode materials.

After performing electrolysis using possible anode materials, graphite was chosen for being inert [52] in the hot (60°C) HCl based electrolyte.

3.3.1 Cathode Choice

For the industrial applications, utilization of collected copper is the second important issue after the recovery of regenerated pickling solution. Therefore, copper [102] was chosen as cathode material for an easier copper utilization. In this case, it was not needed to separate the collected copper from the surface. However, it was found that, working with copper cathodes needs close attention because the hot acid and also its vapor can dissolve copper at a very fast rate when it is not cathodically protected. In order not to introduce a new copper source into the solution from outside, 304 stainless steel cathode [103, 104] was also studied as an alternative material. Stainless steel had a much better resistance to the electrolyte when compared to copper and collected copper could easily be peeled off from the passive surface of this material.

3.3.2 Cathode Preparation

Before starting each experimental run, copper or 304 stainless steel cathode surfaces were prepared to remove dust, oil and solid particles from the cathode surface. The purpose of the treatment was to clean and activate the cathode surface for electrodeposition process to enhance the efficiency of the process and the quality of

the deposit [105]. The cathodes were first exposed to a soap cleaning. Then, hot alkaline cleaning was performed and at last, a very short duration of acidic cleaning was done to remove the oxide film from the surface. The alkaline cleaning was done at 50°C in 0.5 M NaOH solution and the acidic cleaning was done by immersing the cathode material into 50 v/v % HNO₃ solution at room temperature. The cathodes were rinsed in distilled water after each preparation step [106].

In order to be able determine the weight gain, copper cathodes were used in foil form in laboratory scale experiments. The copper foils, to be used as cathode, were weighted after the surface treatment. To maintain the deposition area at 5 cm², 5 cm² of the cathode surface area was dipped into the solution by hanging the cathode from the Teflon lid of the beaker.

However, stainless steel was not available in foil form. Therefore, the weight gains of stainless steel cathodes were examined by measuring the plating thickness using X-Ray Fluorescence (XRF) because a very small weight change on a relatively heavy stainless steel plate could not be measured precisely by weighting. To fix the deposition area at 5 cm², the cathode surface was masked by an adhesive electroplating tape (3M Electroplating Tape 470) after the surface treatment and the open area was exposed to the electrolyte. Using a tape for masking was not possible for copper cathode because the gum from the tape could have left on the cathode which would then change the result of weighting.

3.3.3 Anode Choice

The system has to be comprised of a suitable inert material, not to be dissolved or consumed during the process, as anode [107, 108]. Literature review showed that it was possible to use graphite [103] cermet [108], lead [108], titanium [102] and nickel [109] as anode materials for electrodeposition.

Titanium, lead and graphite anodes were studied as anode candidates at the same experimental conditions. The results of the experiments were characterized by ICP-

MS and XRF. Results of ICP-MS and XRF analyses were evaluated and graphite was chosen as anode material due to its insignificant dissolution.

3.3.4 Anode Preparation

Before starting each experimental run, to remove the dirt from the anode surface, the graphite anode was cleaned with acetone. To fix the surface area and equalize it with the cathode material, the anode material was masked. The masking was performed by the electroplating tape given in section 3.3.2. The surface area of the anode material was maintained at 5 cm² similar to the cathodes.

3.4 Experimental Setup

Three different experimental set-ups were used in this study. The first one was laboratory scale to study electrode reactions, electrode behaviors and collection mechanism of copper.

The second set-up was a pilot scale set-up established at the department of Metallurgical and Materials Engineering Department of METU to test a pilot scale cell using about 200 liters of acid solution for each run.

The third set-up was another pilot scale set-up established at Borçelik Steel plant to run the cell using about 1000 liters of solution for each run.

3.4.1 Laboratory Scale

The experimental setup used in this study is shown in Figure 9, which consisted of a 500 ml beaker used as a batch reactor to hold 300 ml solution. The electrodes were cylindrical graphite anode and a thin foil of copper or a plate of stainless steel cathode. Both anode and cathode had equal effective surface areas of 5 cm². They

were 4.5 cm apart from each other and the operating temperature was 60°C for all experiments.

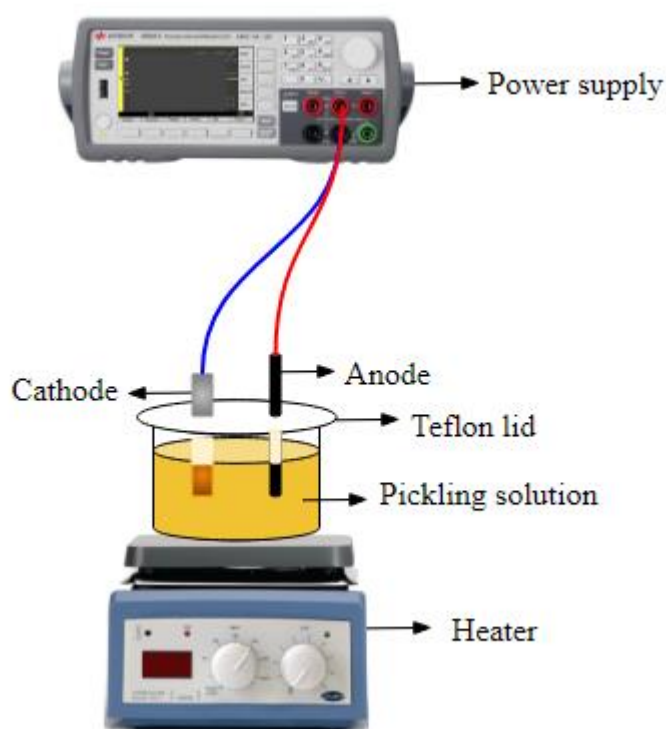


Figure 9. Schematic drawing of experimental setup

The beaker was covered by a Teflon lid to keep the solution volume constant by preventing vaporization during the experiments.

The desired current density was maintained constant during the experiments by Agilent B2901A Precision Source to apply both direct and pulse currents. All of the experiments were performed at 60°C, by a hot plate (Mtops HSD 180), employing a contact thermometer and a magnetic stirrer, which simulated the temperature of the acid used in the steel plant. After each experiment, the electrodes were dried and cathode was examined. The solution samples were transferred to a leak-proof plastic container after each run to perform ICP-MS analyses.

3.4.2 Pilot Plant Scale

For the pilot applications, as a power source, Keysight Technologies N8754A was used to apply direct current and Plating Electronics pe861DA-GD was used to apply pulse current.

3.4.2.1 METU Pilot Plant

After performing the laboratory tests, it was decided to use graphite anode and 304 stainless steel and/or copper cathode for the pilot tests. By using these materials, at first a pilot plant was installed in laboratory of Middle East Technical University. The schematic view of the pilot plant is shown in Figure 10 (a) top and (b) side.

The pilot plant consisted of a collection tank and three tanks with a capacity of approximately 100 liters. The electrolysis tank contained 25 liters of solution and a total of about 200 liters of solution was passed through the electrolysis tank in each run which ensured that the steady state was achieved during the tests.

For the pilot plant tests, two different electrode designs were laid out. The schematic view of the electrode designs for the pilot plant scale is shown in Figure 11. The designs involved flat graphite plate anodes and flat copper and/or 304 stainless steel plate cathodes (a) and cylindrical graphite anodes and s-shaped copper and/or 304 stainless steel cathodes (b).

The total active cathode areas were 0.320 m^2 for plate and 0.385 m^2 for s-shape. The total active area of anodes were 0.320 m^2 for plate and 0.125 m^2 for cylindrical anodes. The ratio of active surface area of anode and cathode for Figure 11 (a) is equal to 1 while the ratio is equal to 0.42 for Figure 11 (b). The plate design was designated for easier operation and the s-shape design was designated to increase the surface area of the cathode.

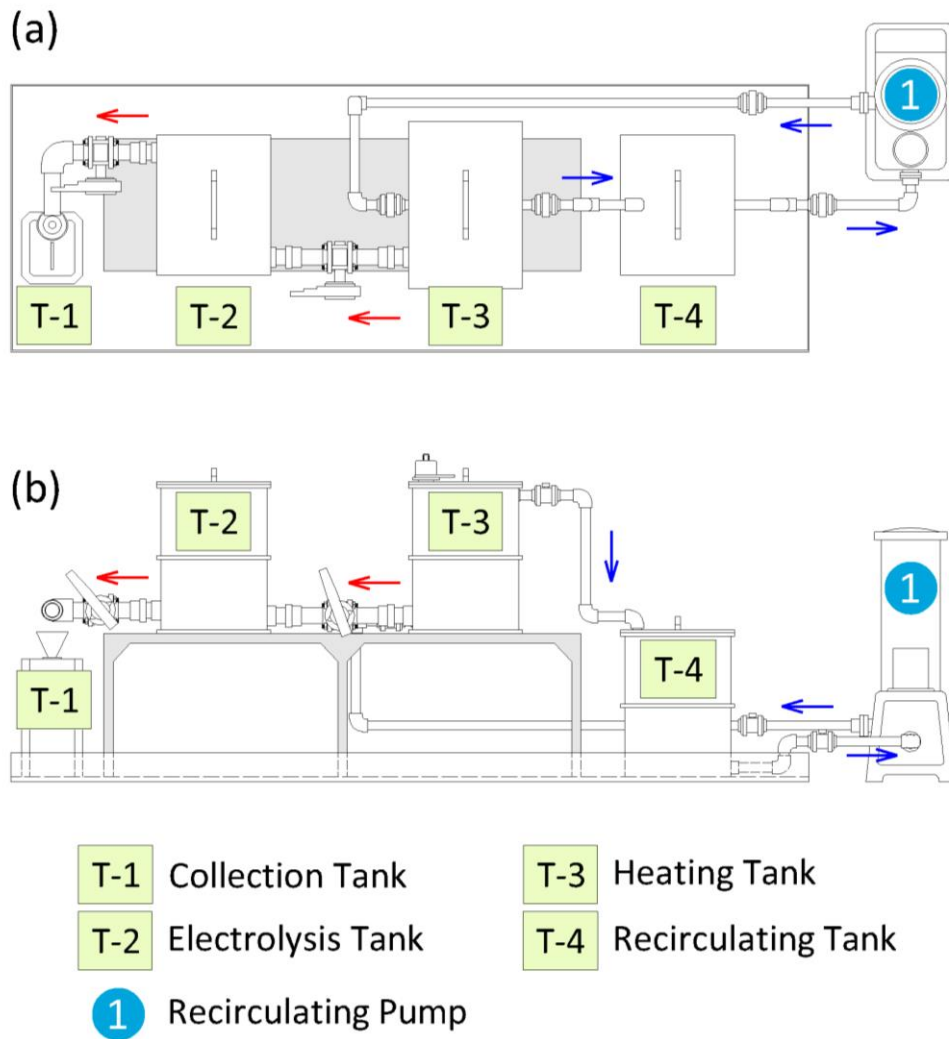


Figure 10. Schematic view of METU pilot plant from (a) top and (b) side

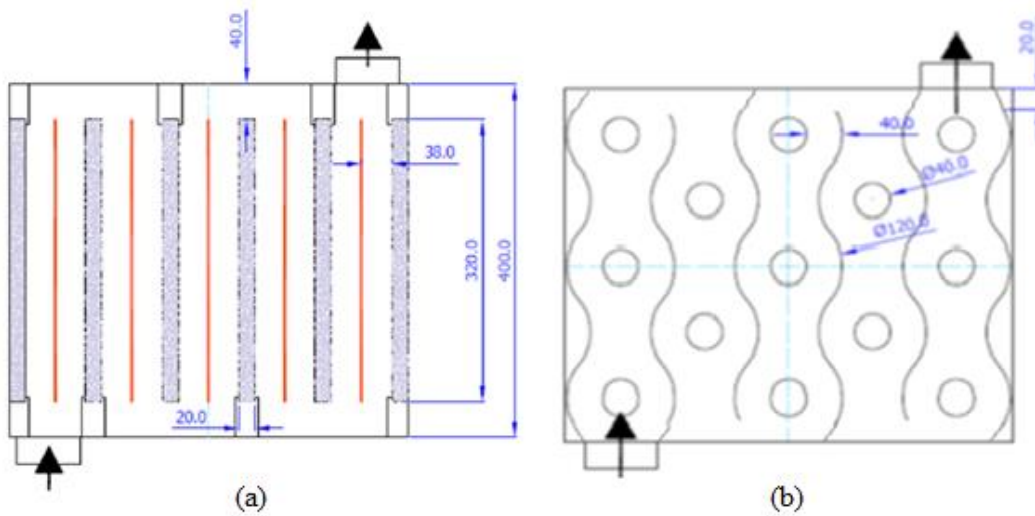


Figure 11. Schematic view of electrode design

3.4.2.2 Borçelik Pilot Plant

The pilot plant setup constructed at Borçelik is shown in Figure 12. The plant consisted of a 1000 liters capacity feeding tank that contained the acid to be electrolyzed, a heating tank to simulate the acid temperature of the steel plant, a 25 liter capacity electrolysis tank where electrodeposition process took place and a 1000 liters capacity collection tank to collect the electrolyzed acid. There were two pumps: one of which was used to circulate the acid between the heaters and feeding tank and the other one, was used to pump the acid from the collection tank when required. The aim of using large feeding and collection tanks were to prolong the electrolysis duration, and the flow rate of the solution was adjusted to 1 L/min.

The tests were performed with only plate anode-cathode design based on the information obtained from METU pilot plant tests. In order to prevent the copper contamination on the edges, corners and sides; the plate cathodes were framed by coating with Teflon. By this way, it was also aimed to prevent the loss of electrodeposited copper.

$$\% \text{ removal} = \frac{(C_i - C_f)}{C_i} \times 100 \quad (20)$$

where C_i and C_f are the initial and final concentrations in parts per million (ppm), respectively.

Parts per million (ppm) is a weight to weight ratio to describe concentrations. It is the mass of a contaminants per million units of total mass. In order to determine the copper concentration, in ppm, in terms of grams, the following equation (21) must be applied.

$$W = C \text{ (ppm)} \times V \text{ (L)} \times \rho \text{ (kg/L)} \quad (21)$$

where W is the total weight of the contaminants, in the solution, in grams, C is the concentration of the contaminant, in the solution, in ppm, V is the volume of the solution in liters and ρ is the density of solution in kg/L as 1.2.

To determine the amount of copper that was deposited, analysis was done on the cathode. Precision scale measurements were performed on copper cathodes, and XRF analyses were performed on stainless steel cathodes. The amount of copper deposited on copper cathodes were determined from the difference between the initial and the final weights of the cathode. However, the amount of copper deposited on the stainless steel cathodes were calculated according to the formula given in equation (22).

$$m = t \times A \times \rho \times 10^{-4} \quad (22)$$

where m is the mass of the deposited copper in grams, t is the thickness of the deposition determined by XRF measurements in microns (μm), A is the deposition area in centimeters square and ρ is the density of copper in g/cm^3 as 8.96.

3.6 Experimental Design

The operation variables were determined as initial copper concentration, current density, electrolysis duration, and current type. For the determination of effect of

initial copper concentration, 50, 100 and 200 A/m² current densities were applied to the solutions containing 85, 127 and 154 ppm initial copper concentrations. But, the effect of current density, electrolysis duration and current type were studied by using the levels shown in Table 2.

For the pulse current applications, 5 ms on time (t_{on}) and 5 ms off time (t_{off}) were applied on the system. Therefore the average current densities were shown in Table 2 for the pulse current applications. The average current density (I_{avg}) that was applied on the system was calculated by using equation (18).

The experimental route was obtained by the full factorial experiment design. According to the full factorial experiment design, 18 experiments should be performed per cathode material as given in Table 3.

Table 2. Independent variables and their levels

Independent Variables	<i>Level 1</i>	<i>Level 2</i>	<i>Level 3</i>
Current Density (A/m ²)	100	150	200
Electrolysis Duration (h)	2	4	6
Current type	Direct Current	Pulse Current	

After performing the experiments, the results were written to the chart and the graphs and performed statistical analyses were created by the Minitab® software [110,111]. With the help of this software, results for the test conditions can be predicted without performing any new experiments. pH and conductivity of the acid and the amount and morphology of the deposition were determined as response variables.

Table 3. Full factorial design of experiments

Run Order	<i>Current Density</i> (A/m^2)	<i>Electrolysis Duration</i> (<i>h</i>)	<i>Copper Concentration</i> (<i>ppm</i>)
1	200	6	DC
2	200	2	PC
3	200	4	PC
4	150	2	DC
5	150	2	PC
6	100	6	DC
7	100	2	DC
8	150	4	PC
9	100	6	PC
10	100	2	PC
11	150	6	DC
12	200	2	DC
13	100	4	PC
14	150	4	DC
15	150	6	PC
16	200	4	DC
17	200	6	PC
18	100	4	DC

CHAPTER 4

RESULTS AND DISCUSSION

4.1 Determination of Current Density

Graphite anode and copper cathode were used in the initial experiments. Before starting the experiments, linear sweep voltammetry analysis was performed on copper containing regenerated pickling solution of the steel plant and corresponding blank solution at 60 °C.

Figure 13 shows the linear sweep voltammogram of both of the solutions. From the examination of the figure, potentials and corresponding current densities for the electrode reactions could be picked up. As can be seen in Figure 13, there was an anodic current before the voltage was applied because of the dissolution of copper into the electrolyte in this extremely corrosive environment of blank solution. At around -0.5 V potential difference between anode and cathode, the first cathodic reaction started and gave a clear reduction peak at about -0.7 V in the case of regenerated pickling solution. This peak was attributed to the reduction of Cu^{+2} to Cu^+ . When the cathodic potential was further increased, a second reduction peak was obtained at around -1.5 V, which was thought to be originated from the reduction of Cu^+ to solid Cu [101]. Potentials more negative than -1.5 V resulted in too much H_2 evolution at the working electrode. Furthermore, it was observed that higher current densities resulted in a fast and discontinuous powder deposition together with the decreased efficiency due to the inevitable H_2 evolution at the cathode and the Cl_2 evolution at the anode [76].

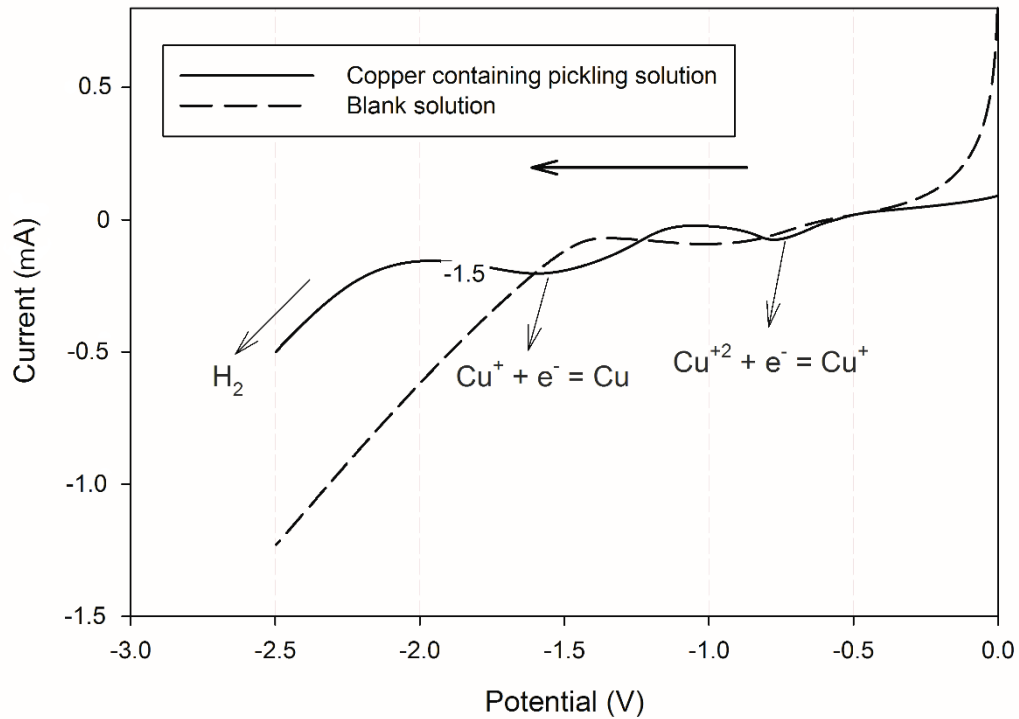
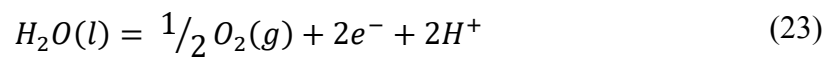


Figure 13. Linear sweep voltammetry of copper containing regenerated pickling solution and corresponding blank solution at a scan rate of 25 mV/s using 1.5 cm² electrode area

Therefore, it was decided to operate the electrochemical cell between -0.5 and -1.5 V to include both electrode reactions. Furthermore, it was aimed to obtain smooth copper deposition at the cathode without too much H₂ evolution. These voltages corresponded to a current density range from 50 to 200 A/m².

At this range, the electrode reactions were reduction of copper (equation (7)) and hydrogen evolution (equation (17)) at the cathode, and evolution of oxygen at the anode as given in equation (23).



4.2 Choice of Electrodes

4.2.1 Choice of Anode Material

At the beginning of the laboratory scale experiments, titanium, lead and graphite were tested as anode materials and they were matched with copper and 304 stainless steel cathodes. The electrolysis experiments were performed on regenerated pickling solution at 60°C on equal active electrode areas. The cathode materials were immersed into the solution while applying a constant voltage between anode and cathode to prevent them from chemical attack. The electrolysis experiments were performed at the same electrolysis duration (4 hours), current density (100 A/m²) and initial copper concentration (145 ppm) for both cathodes against the three different anode materials.

After the electrodeposition process, the deposited samples together with the electrolytes were characterized. When ICP-MS analyses of the electrolyzed solutions were examined, it was observed that both copper and stainless steel cathodes could remove copper from the hot regenerated pickling solution.

From the analysis of ICP-MS results, the anode materials were sorted in terms of copper removal from more to less as; titanium, lead and graphite for both of the cathodes. For the copper cathode, the level of copper was reduced by 28.9 %, 26.2 % and 25.5 % when titanium, lead and graphite anodes were used, respectively. In the case of stainless steel; copper level, calculated by the equation (20) was reduced by 35.9 %, 31.0 % and 28.3 % when titanium, lead and graphite anodes were used, respectively. The change in copper concentration in ppm for (a) copper and (b) stainless steel cathode are shown in Figure 14.

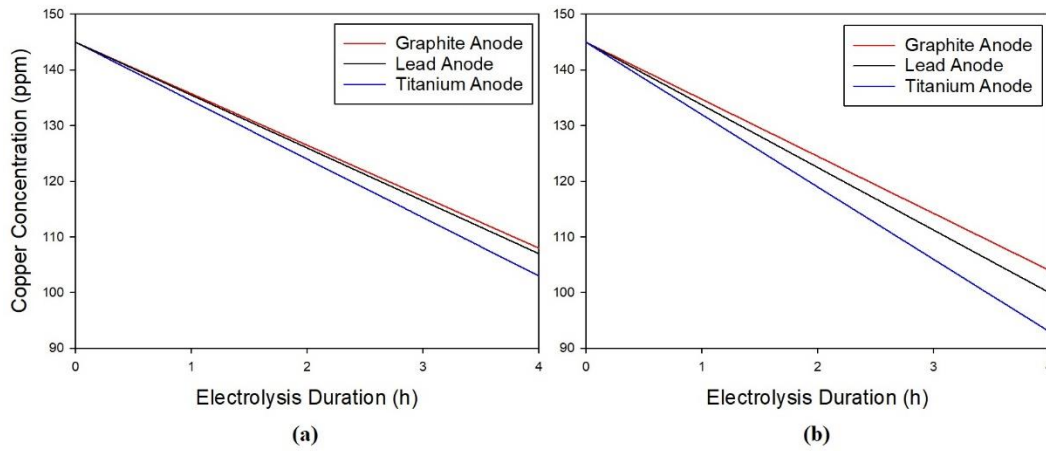


Figure 14. Change in copper removal for (a) copper and (b) stainless steel cathodes

From the visual examination of the cathodes, it was seen that brighter surfaces were obtained from the experiments employing titanium anode as shown in Figure 15.

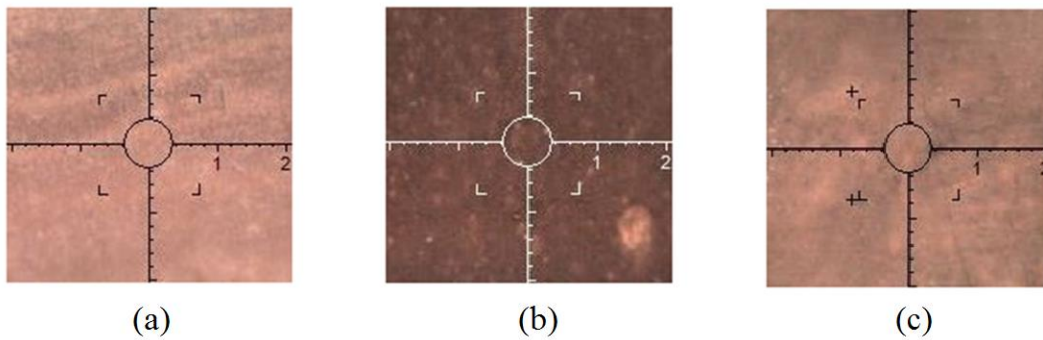


Figure 15. Visual examination of stainless steel cathodes used against (a) titanium, (b) lead and (c) graphite anodes

The measured weights of deposited copper, by precision scale, were 10.8, 6.7 and 5.6 mg for titanium, lead and graphite anodes, respectively when copper was used as cathode material. The results were 10.5, 9.5 and 9.2 mg with respect to the ICP-MS analysis.

The measured thicknesses by XRF were 1.345, 1.096 and 0.857 μm for titanium, lead and graphite anodes, respectively when stainless steel was used as cathode material. The thickness results were given by taking the average of randomly selected 16 points from all over the cathode surface. Due to the thickness results the weight of the copper deposited on the stainless steel surface was 6.03, 4.91 and 3.84 mg as for titanium, lead and graphite anodes, respectively calculated by the equation (22). The results were 13.0, 11.2 and 10.2 mg with respect to the ICP-MS analysis. When the precision scale and ICP-MS analysis results were compared for both of the cathodes, the results were not the same but gave the similar relative tendency.

From the results, it was observed that more copper removal was obtained from the experiments employing titanium anode and the efficiency of stainless steel cathode was more than the copper cathode. However, it was observed that titanium and lead anodes released large amounts of titanium and lead ions into the solution as shown in Figure 16. The levels of titanium and lead increased from almost 0 to 700 and 2800 ppm for copper cathode experiments and 716 and 2600 ppm for stainless steel cathode experiments when they were used as anodes in the corresponding experiments.

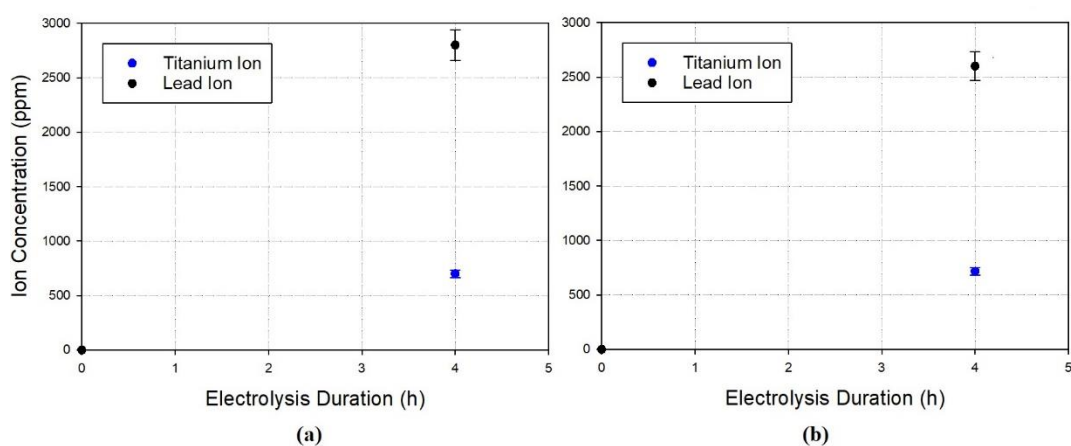


Figure 16. Release of titanium and lead ions for the experiments carried out with Titanium and Lead anodes using (a) copper and (b) stainless steel cathodes

These results were in accordance with the studies which reported corrosion of lead [112] and titanium [112–114] in concentrated HCl solutions at room temperature. The corrosion rates were even higher in this study because these materials were used as the anode of an electrochemical cell and their potentials were further increased. This leads to metal contamination in the pickling solution, material loss from the anode and efficiency decrease in the pickling process. Therefore, graphite was selected as the best anode material in the electrochemical treatment of copper from regenerated pickling solutions based on no detectable anode dissolution.

As a result, working with titanium and lead anodes were deemed unsuitable and it was decided to use graphite anodes.

4.2.2 Choice of Cathode Material

The choice of cathode material was important to ensure a proper adhesion for effective copper removal and its utilization. In order to test the adhesion behavior; titanium, 304 stainless steel and copper were tested as cathode materials. It was observed that when working with titanium cathode, the collected copper could not hold onto the surface and could be returned to the solution and/or swept with a small flow. At the same time, it was not a cost effective material selection.

The copper cathode was studied for an easier copper utilization because there is no need for scrapping off the deposit from the electrode. When the electrodes are loaded to a certain level, they can be melted together with the deposited copper. Copper is prone to oxidation by hot acid and its vapor, so it was hard to manage the copper cathode assembly. The cathode was protected by applying a constant voltage between the electrodes while immersing it into the solution. After the cathode was completely immersed in the solution, the selected constant current was applied. It was observed that copper electrodes were severely corroded especially above the electrolyte level by hydrochloric acid gas in 6 hours long experiments.

For the above mentioned problems of copper cathode, stainless steel was also tested as the cathode material because of its higher corrosion resistance. The thin chromium oxide layer at the stainless steel surface provided adequate adhesion between the deposit and the electrode which kept the deposit on the electrode under the influence of the applied potential but prevented very good adhesion. Therefore, the deposit could easily be peeled off from the electrode when it was taken out of the electrolyte.

It was easier to manage stainless steel cathode at the beginning of the electrolysis. After some time of electrolysis, the stainless steel cathode was covered with copper and the rest of the electrolysis can be considered as copper plating onto copper. Therefore, the rest of the electrolysis experiments were the same as those with copper cathodes except that there was no copper left outside the pickling solution to be affected from the vapor of the acid. Utilization of the collected copper required a secondary process to separate the copper from the stainless steel cathode. When the deposit was separated from the surface, the stainless steel cathode could be used again.

It was observed that deposition onto stainless steel and copper cathodes could be successfully achieved and the collected copper adhered to the surface. Therefore, priority was given to the stainless steel cathode due to easier maintenance.

4.3 Choice of Pickling Solution

For the study, it was possible to work on both spent pickling solution and regenerated pickling solution. However the literature review results showed that working on regenerated pickling solution is more efficient than working on spent pickling solution due to the content of ferrous and non-ferrous metal ions [98–100].

The morphology of the deposition and current efficiency varies with the type of pickling solution. In the presence of other metals, the morphology of the deposition differs. The studies also showed that, during the copper electrowinning from dilute solutions, the current efficiency decreases proportionally with increasing ferric ion

concentration in the solution [97, 99, 100]. For this reason, working on regenerated pickling solution instead of spent pickling solution is more efficient. Nevertheless, removal of copper was studied on both of the solutions.

The comparison between the results of regenerated and spent pickling solutions are shown in Figure 17. The tests were done under the same experimental conditions (current densities of 50, 100, 150 and 200 A/m² and electrolysis durations of 2, 4 and 6 hours) but with different current characteristics (direct and pulse current methods). Since the impurities in the spent pickling solution were an obstacle to the collection of copper, amount of the deposited copper was lower than regenerated pickling solution tests.

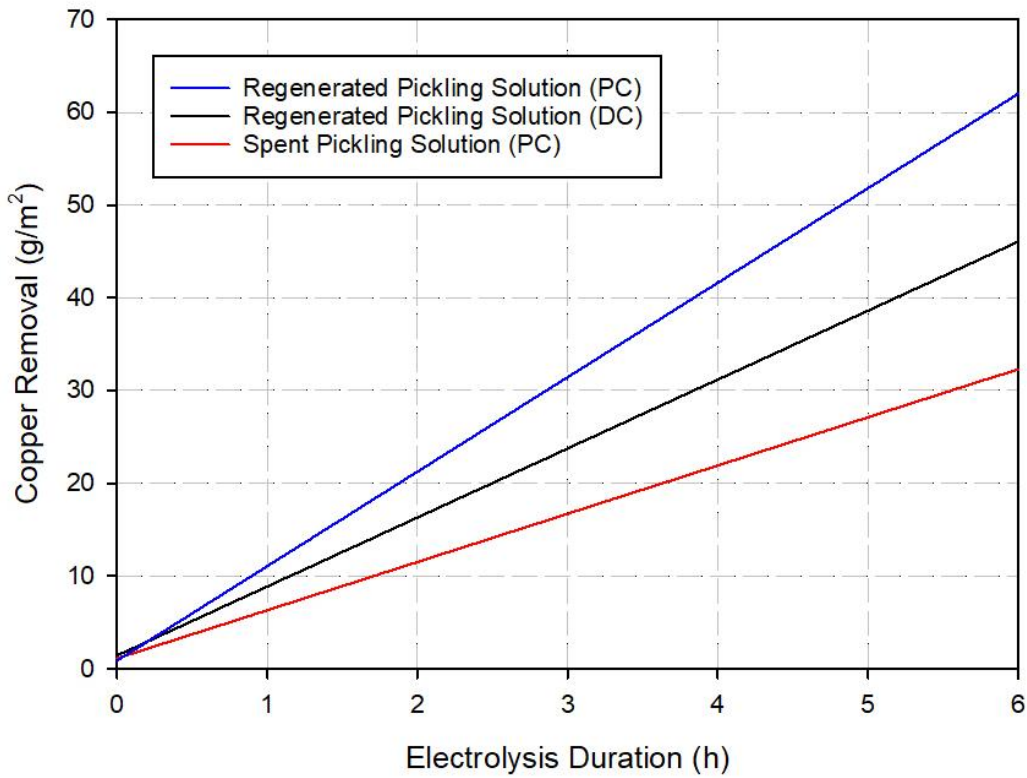


Figure 17. Comparison of copper removal of regenerated and spent pickling solution

These results were obtained using stainless steel cathode. When the other parameters were kept constant, pulse current was more effective than direct current at the same average current density. Therefore, pulse current was applied during removal of copper from spent pickling solution and it was concluded that copper removal from regenerated acid provided better results.

4.4 Effects of Electrolysis Parameters

The effects of initial copper concentration, current density and electrolysis duration on copper removal were investigated. Effect of current density and electrolysis duration was investigated by a full-factorial experiment design as given in Table 3.

The figures in the following sections are showing the main effects. For the examination of ‘effect of initial copper concentration’, average of 9 experiments were used for each point and all 27 results were used in the construction of each line/curve of the plot [110, 111]. For the analysis of other electrolysis parameters, the three current densities and electrolysis durations given in Table 2 were studied. However, only one initial copper concentration, 127 ppm, was used. As a result, in the construction of the figures showing the results of experiments, 3 data were involved for each point and 9 data were involved in each line/curve of the plots. The error bars in the following figures were used to indicate the uncertainty in ICP-MS measurements. This choice of presentation was made to derive statistical conclusions from small amount of copper collected from strong acidic solution containing very low copper concentrations.

4.4.1 Effect of Initial Copper Concentration on Copper Removal

The main effect of initial copper concentration of regenerated pickling solution on copper removal was examined only for the copper cathode and using direct current. Direct current densities of 50, 100 and 200 A/m² applied to the solutions containing 85, 127 and 154 ppm initial copper concentrations. The results obtained by the ICP-

MS analyses are given in Figure 18. As shown in Figure 18, as the copper concentration in the solution increases, it is easier to collect copper from the solution due to the increase in the copper ion activity. The error lines shown in Figure 18 is the possible 5% error margin from ICP-MS measurements.

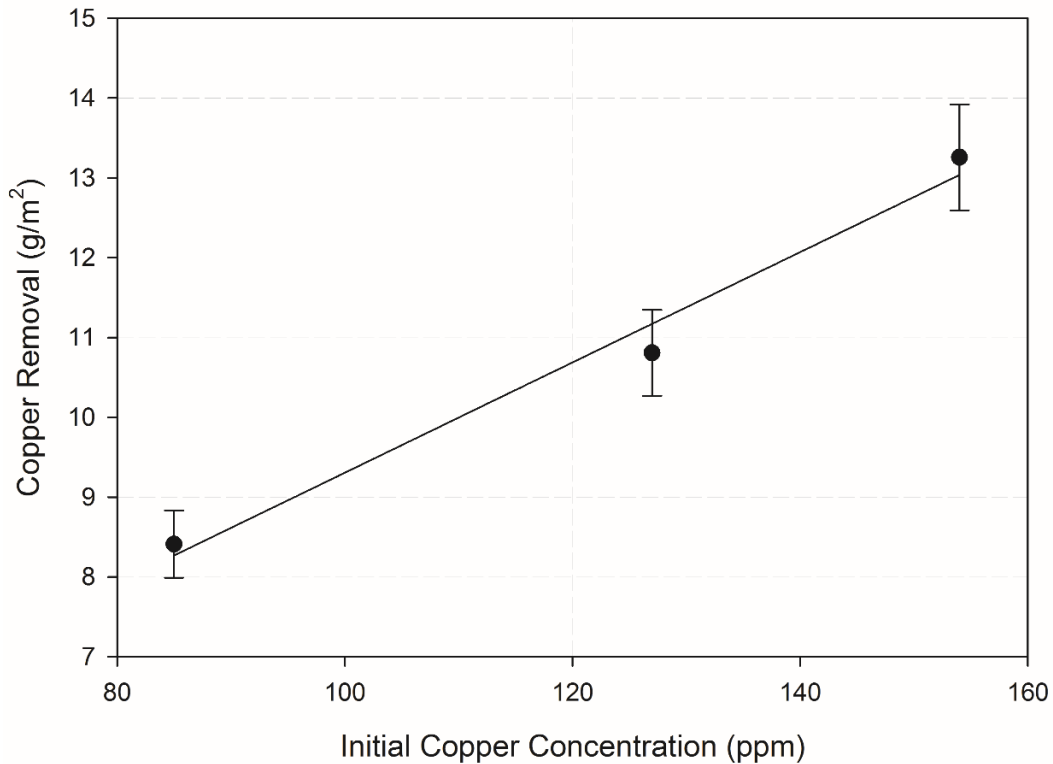


Figure 18. Main effect of initial copper concentration of the regenerated pickling solution on copper removal

Removal of 1 mg/cm² of copper corresponds to a decrease of approximately 14 ppm in copper concentration of the regenerated pickling solution when the area of the cathode and the volume (total weight) of the acid used in this study were taken into consideration.

Despite immersion of the copper cathode into the solution by applying current on it, the challenges pushed to repeat the experiments using stainless steel cathode. After

this point, initial copper concentration of the electrolyte was fixed at 127 ppm. In order to accelerate the copper deposition, pulse current method was also used.

4.4.2 Effect of Current Density and Current Characteristics on Copper Removal

The main effect of current density of regenerated pickling solution on copper removal was examined for both copper and stainless steel cathodes using direct and pulse current methods. The experimental results that were obtained by the ICP-MS analyses were evaluated for direct current method in Figure 19 (a) and pulse current method in Figure 19 (b) using both copper and stainless steel cathodes.

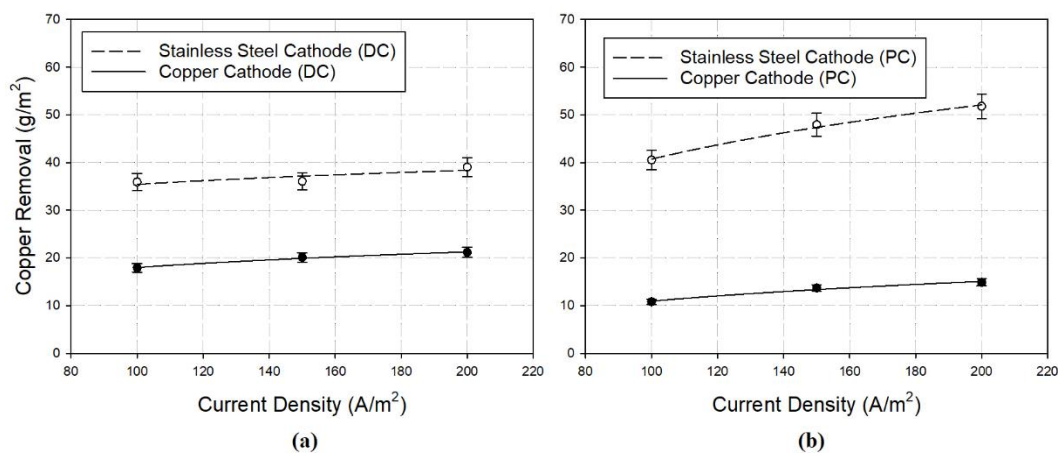


Figure 19. Main effect of current density on copper removal by (a) direct current method and (b) pulse current method for copper and stainless steel cathodes

In the graphs given in Figure 19, the effect of current density was studied for three levels of current density and three levels of electrolysis duration using 127 ppm initial copper concentration by direct and pulse current methods. Each point in the graphs is obtained by averaging 3 experiments and each line is drawn by averaging 9 experiments conducted at different electrolysis durations according to Table 2.

As it can be deduced from Figure 19, copper removal increased with increasing current density. When the results of cathodes are compared, it was observed that the amount of copper removal was higher for the stainless steel cathode regardless of the current form used.

As can be seen, under the same experimental conditions, direct current method was more efficient than pulse current method for copper cathode contrary to expectation. The reason for this might be the difficulty of protecting the copper cathode from dissolving in the pickling acid, especially when the solution was hot under of current conditions. Therefore, the current was applied to the cathode before it was immersed into the solution. However, current was switched off for short time durations during the pulse current application. The pulse current probably could not compensate the amount of dissolution of collected copper from the copper cathode. It was also observed that pulse current method was more efficient than direct current method for stainless steel cathode under the same experimental conditions. Regardless of the type of the current method, dust formation was observed on the cathode surface as the current density was increased.

4.4.3 Effect of Electrolysis Duration on Copper Removal

The main effect of electrolysis duration on copper removal was examined for both copper and stainless steel cathodes and direct and pulse current methods. Experimental results that were taken from the ICP-MS analyses were evaluated for direct current method in Figure 20 (a) and pulse current method in Figure 20 (b) for both copper and stainless steel cathodes. The effect of electrolysis duration was examined for three levels of current densities and three levels of electrolysis durations using 127 ppm initial copper concentration.

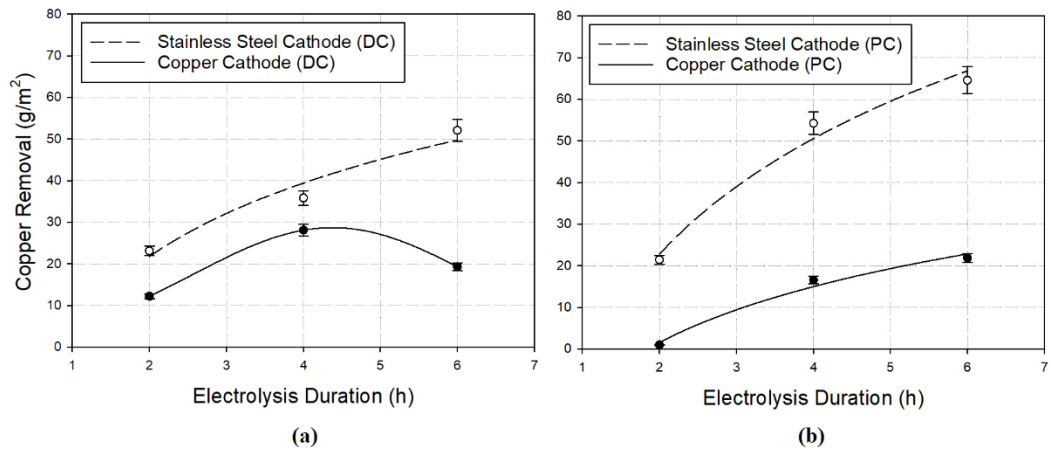


Figure 20. Main effect of electrolysis duration on copper removal by (a) direct current and (b) pulse current method for copper and stainless steel cathodes

As can be seen in Figure 20 (a), a greater amount of copper was removed by direct current as a result of increasing electrolysis duration when stainless steel cathode was used. But copper removal decreased after 4 hours of electrolysis due to the copper dissolution problem when copper cathode was used. It is because copper cathode can also be affected by the HCl vapor. Therefore, as the cathode could not be protected from the acid vapor, dissolution occurred with increasing electrolysis duration.

As can be seen in Figure 20 (b), a greater amount of copper was removed as a result of increasing electrolysis duration with pulse current application. When the results of cathodes are compared, it was observed that the amount and rate of copper removal of stainless steel was more than the copper cathode for both current methods. It is because maintaining the stability and repeatability in the experiments were much more difficult with the copper cathode due to the interaction of copper by the HCl and its vapor.

It can be seen that copper removal using pulse current method was less effective than that of direct current method when copper cathode was used because it is very difficult to protect the copper cathode without dissolving in the hot pickling solution.

However, pulse current method may become more effective than direct current method when the steady state is achieved. The amount of copper removal for pulse current method was more than the direct current method under the same experimental conditions when stainless steel cathode was used. Regardless of the type of the current method, dust formation was observed on the cathode surface as the duration of the test was increased in the case of high current densities.

4.5 COMSOL Multiphysics Analyses

COMSOL Multiphysics modeling and analysis were performed for the pilot plant in order to have an idea before the application. The applied current density on the system was set as 150 A/m^2 direct current. Total cathode area according to pilot was 0.32 m^2 . According to the solution shown in Figure 21, after 6 hours of electrolysis, the majority of the deposition reached a thickness of 120 microns. The corners were thicker than the surface due to the edge effect. The scale in Figure 21 is based on 100% current efficiency.

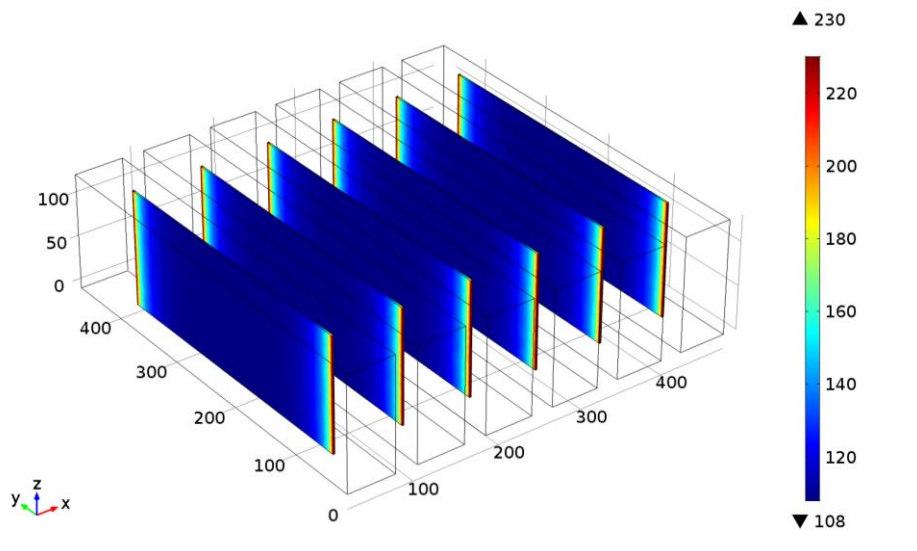


Figure 21. The results of COMSOL multiphysics solution of designed pilot plant showing total electrode thickness change after 6-hours of electrolysis

Using laboratory test results, the expected pilot scale results for regenerated pickling solution were calculated for both copper and stainless steel cathodes, using direct and pulse current methods and plate and s-shape cathodes. Laboratory tests were performed on 5 cm² active cathode area and 300 cm³ acid solution. It was planned to use 25 liters electrolyte in the pilot plant. When the height of the electrodes were considered as 10 cm, total active cathode area for the plate cathodes come out as 0.320 and for the s-shape as 0.385 m². This means, in pilot plant application, the active cathode area will be 640 times more for plate and 770 times more for the s-shape than laboratory application. Therefore, the amount of collected copper from the pilot plant will be 640 and 770 times more than the laboratory applications. While copper was collected from 300 cm³ solution in the laboratory, the indicated amounts will be collected from 192 and 231 liters of solution in the pilot.

Table 4 show the expected pilot results based on the laboratory results for both plate and cylindrical anodes. The flow rate required to remove 25% of copper is calculated by equation (24).

$$\vartheta_{25} = \vartheta \times \frac{(\% \text{ removal})}{25} \quad (24)$$

where ϑ is the calculated flow rate and (% removal) is the experimentally collected copper percent (Cu amount) in the laboratory.

Table 4. Table of pilot plant expectations based on laboratory studies

Laboratory Results					<i>Pilot Expectation</i>			
Cathode (Cu/SS)	Current Method (DC/PC)	Current Density (A/m ²)	Electrolysis Duration (h)	Copper Removal (%)	<i>Plate Anodes</i>		<i>Cylindrical Anodes</i>	
					<i>Flow Rate (L/h)</i>	<i>Flow Rate for 25% Cu Removal (L/h)</i>	<i>Flow Rate (L/h)</i>	<i>Flow Rate for 25% Cu Removal (L/h)</i>
Cu	DC	100	2	4.7	96	18.1	116	21.8
Cu	DC	100	4	38.5	48	74.1	58	89.1
Cu	DC	100	6	18.9	32	24.2	39	29.1
Cu	DC	150	2	15.7	96	60.5	116	72.8
Cu	DC	150	4	24.4	48	46.9	58	56.4
Cu	DC	150	6	26.7	32	34.3	39	41.2
Cu	DC	200	2	19.7	96	75.6	116	90.9
Cu	DC	200	4	29.1	48	55.9	58	67.3
Cu	DC	200	6	18.1	32	23.2	39	27.9
Cu	PC	100	2	13.3	96	51.0	116	61.4
Cu	PC	100	4	24.2	48	46.5	58	56.0
Cu	PC	100	6	-2.3	32	-3.0	39	-3.6
Cu	PC	150	2	-23.4	96	-90.0	116	-108.3
Cu	PC	150	4	7.8	48	15.0	58	18.1
Cu	PC	150	6	60.2	32	77.0	39	92.6
Cu	PC	200	2	13.3	96	51.0	116	61.4
Cu	PC	200	4	21.9	48	42.0	58	50.5
Cu	PC	200	6	13.3	32	17.0	39	20.4

Continued table of pilot plant expectations based on laboratory studies

Laboratory Results					<i>Pilot Expectation</i>			
Cathode (Cu/SS)	Current Method (DC/PC)	Current Density (A/m ²)	Electrolysis Duration (h)	Copper Removal (%)	<i>Plate Anodes</i>		<i>Cylindrical Anodes</i>	
					<i>Flow Rate (L/h)</i>	<i>Flow Rate for 25% Cu Removal (L/h)</i>	<i>Flow Rate (L/h)</i>	<i>Flow Rate for 25% Cu Removal (L/h)</i>
SS	DC	100	2	28.1	96	108.0	116	129.9
SS	DC	100	4	32.8	48	63.0	58	75.8
SS	DC	100	6	56.3	32	72.0	39	86.6
SS	DC	150	2	15.6	96	60.0	116	72.2
SS	DC	150	4	46.9	48	90.1	58	108.3
SS	DC	150	6	55.7	32	70.0	39	84.2
SS	DC	200	2	31.3	96	120.0	116	144.4
SS	DC	200	4	37.5	48	72.0	58	86.6
SS	DC	200	6	58.6	32	75.0	39	90.2
SS	PC	100	2	14.8	96	57.0	116	68.6
SS	PC	100	4	53.9	48	105.5	58	124.5
SS	PC	100	6	64.8	32	83.0	39	99.9
SS	PC	150	2	26.6	96	102.0	116	122.7
SS	PC	150	4	60.2	48	115.5	58	139.0
SS	PC	150	6	69.5	32	89.0	39	107.1
SS	PC	200	2	30.5	96	117.0	116	140.8
SS	PC	200	4	62.5	48	120.0	58	144.4
SS	PC	200	6	75.8	32	97.0	39	116.7

When the plate electrodes were used; the required flow rate was found in average as 62 L/h and the corresponding value for cylindrical anodes was 75 L/h for 100, 150 and 200 A/m² current density.

4.5.1 Evaluation of METU Pilot Results

Laboratory tests showed that pulse current method is more efficient than direct current method. Therefore, pilot tests were continued with pulse current method. In the pilot tests, cathodes were protected by applying a constant voltage between anodes and cathodes to solve the copper dissolution problem while immersing into the solution. After the cathodes were completely covered by the solution, application of pulse current was started. The electrolysis starts and copper content of the solution decreases when it is possible to give the desired current value. The samples were taken every 5 minutes during the electrolysis.

The first demonstrated pilot plant showed that, when the level of the electrolysis tank changed, the results fluctuated. The level of the electrolyte was changing due to the variations of input and output flow flow rates caused by changes in pressure heads of the electrolyte. The fluctuations were mainly observed in the studies performed by using copper cathodes due to the copper dissolution. Therefore, changes in solution were investigated when there was no copper dissolution from electrodes.

Figure 22 compares the efficiency and fluctuation behavior of copper and stainless steel cathodes at 100 A/m^2 current density with time using pulse current method.

According to the study done with copper cathode; electrolysis started at 153 ppm initial copper concentration and reached steady state condition nearly at 135 ppm. It was determined that approximately 11.5% of the total copper of the solution could be collected under these conditions.

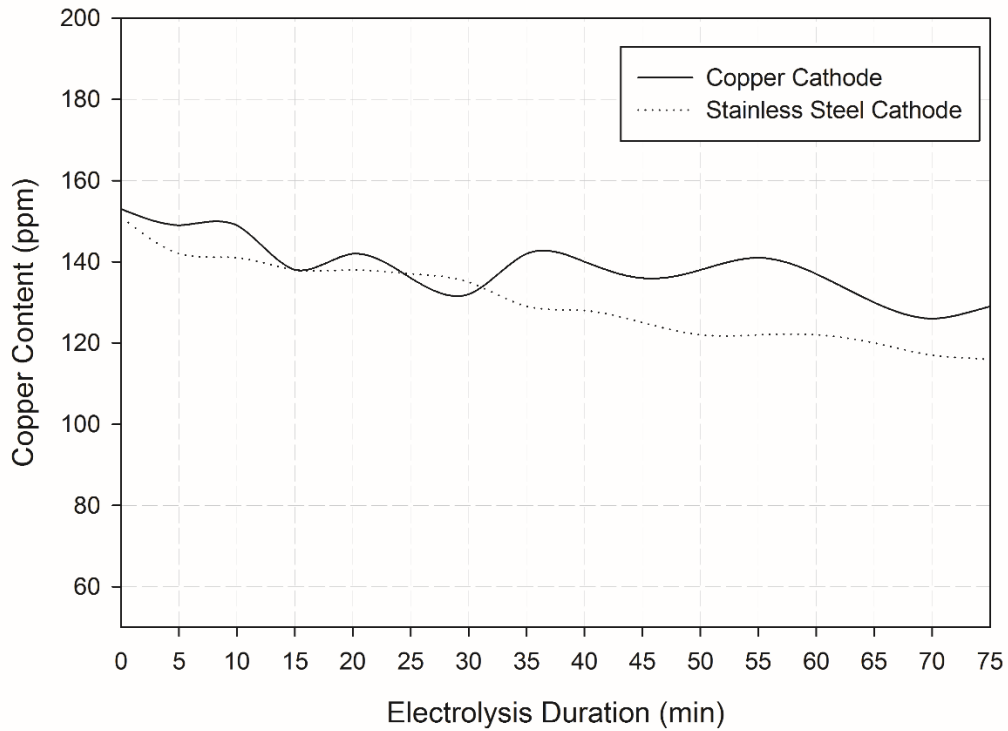


Figure 22. Change in copper content with time for a current density of 100 A/m² with plate copper and stainless steel cathodes

According to the study done with stainless steel cathode; electrolysis started at 151 ppm initial copper concentration and reached steady state condition nearly at 122 ppm. It was determined that approximately 18.9% of the total copper of the solution could be removed under these conditions. When the two cathodes were compared, it was observed that stainless steel cathodes were more efficient than copper cathodes as in the laboratory tests.

As it was decided to use stainless steel cathode, in order to prove the effect of current method in pilot plant, s-shape cathodes were also tested at the same current density by pulse and direct current methods. Figure 23 shows the comparison of current methods for collecting copper as a function of electrolysis duration for s-shape stainless steel cathodes at 130 A/m² current density.

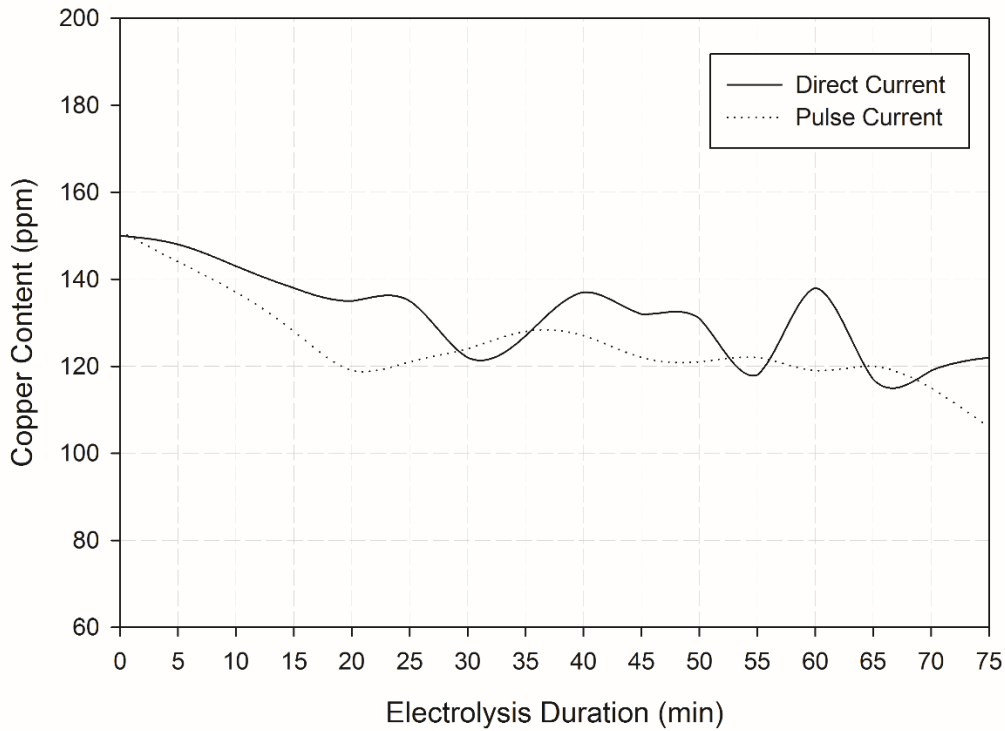


Figure 23. Comparison of current method with respect to electrolysis duration for s-shape stainless steel cathodes at 130 A/m² current density

From the analysis of the study done using 130 A/m² pulse current method, it can be seen that the electrolysis started at 151 ppm initial copper concentration and reached the steady state condition nearly at copper concentration of 120 ppm. Referring to the conditions, it was determined that approximately 20.5% of total copper could be removed from the system. On the other hand, the electrolysis started at 150 ppm initial copper concentration and reached the steady state condition nearly at 126 ppm copper concentration for direct current application. This corresponded to approximately 16% copper removal. When the two methods are compared, it was observed that pulse current method is more efficient than direct current method as in the laboratory tests.

After deciding to use stainless steel cathode by employing pulse current method, in order to see the effect of cathode shape, plate and s-shape stainless steel cathodes

were used to remove copper by pulse current method at 130 A/m^2 current density. Figure 24 shows the comparison of cathode shape with respect to electrolysis duration at 130 A/m^2 current density.

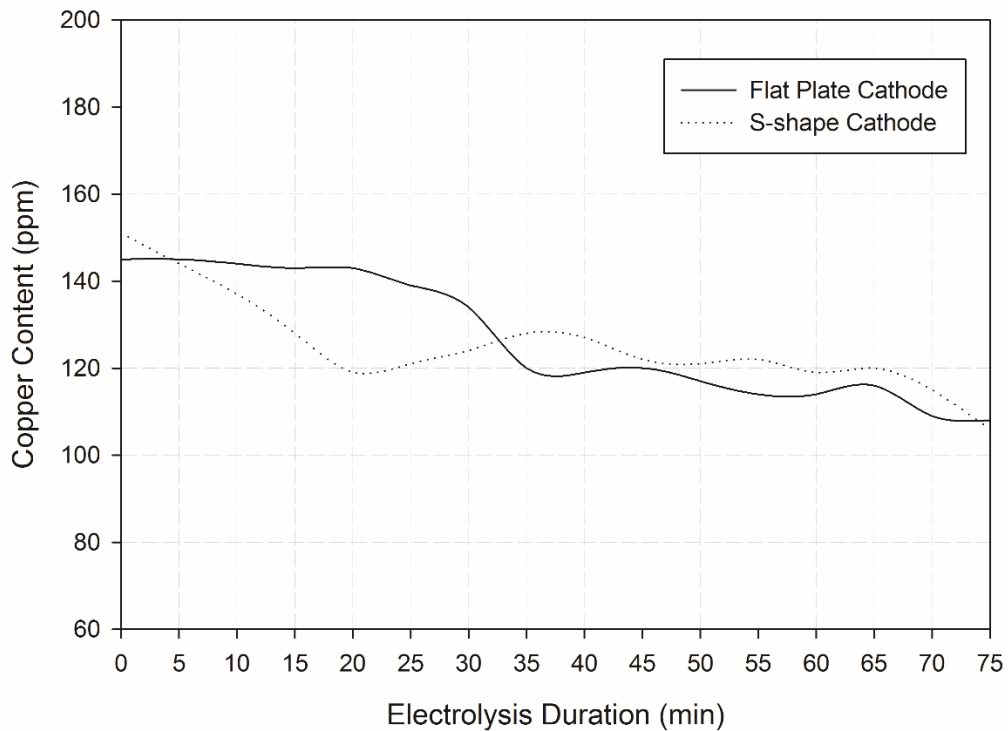


Figure 24. Comparison of cathode shape with respect to electrolysis duration at 130 A/m^2 current density

As can be seen in Figure 24, the electrolysis started at 151 ppm copper concentration and reached the steady state condition nearly at copper concentration of 120 ppm for s-shape cathodes. Referring to the conditions, it was determined that approximately 20.5% of total copper could be removed from the system. In the case of plates, the electrolysis started at 145 ppm copper concentration and reached the steady state condition nearly at copper concentration of 117 ppm. Therefore, approximately 19.2% of total copper could be removed from the solution. From the comparison of different cathode shapes, it was observed that s-shape cathode can remove more

copper than plate cathode. But the difference is negligible when the difficulty of production and operation of s-shape cathode is taken into consideration.

In order to prove the effect of current density on copper removal, pilot plant was operated at different current density values. The system was operated by pulse current method at 100, 130 and 180 A/m² average current densities. Figure 25 shows the comparison of the effect of current density on stainless steel plate cathode.

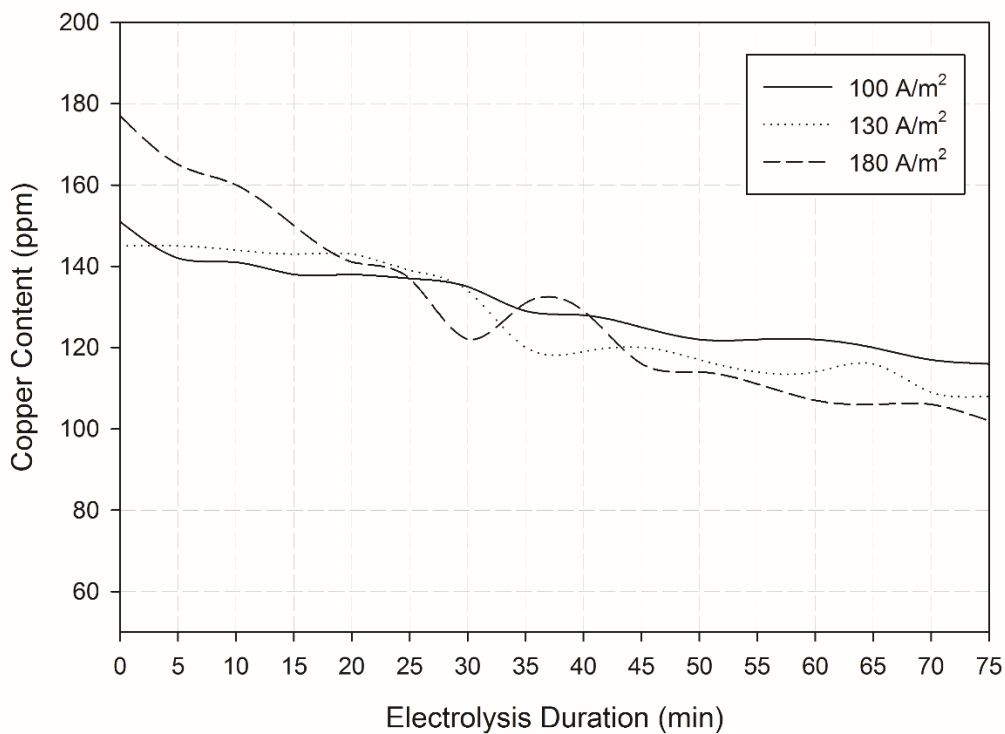


Figure 25. Comparison of effect of current density on stainless steel plate cathode

As can be seen in Figure 25, initial copper concentration values were different in the experiments. The steady state was achieved at 122, 117 and 109 ppm for the experiments at 100, 130 and 180 A/m² average current density, respectively. These values corresponded to 18.9% copper recovery for the experiment at 100 A/m², 19.2% for 130 A/m² and 38.5% for 180 A/m².

When the effects of current densities are compared, it was observed that 180 A/m² current density seemed more effective. But from the laboratory scale experiments it was also observed that, copper removal increased with increasing initial copper concentration and increasing current density resulted in side reactions therefore, the optimum current density was found as 130 A/m².

4.5.2 Evaluation of Borçelik Pilot Plant

As a result of the pilot tests conducted at METU, the possibility of copper removal was proven. In order to maintain the study for a longer period and ensure steady state, feeding and storage tanks with a capacity of 1000 liters were installed within Borçelik and pilot tests were continued there.

The tests were started by using 100 A/m² average pulse current density on plate electrode design. The amount of copper in the solution with respect to electrolysis duration is given in Figure 26. Copper concentration decreased from 182 to 141 ppm which corresponded to about 22.6 % copper removal. The level was not enough but close to the purpose of the study. It should be noted that the solution could be passed from the electrolysis line once again, which would decrease the copper level close to 100 ppm level.

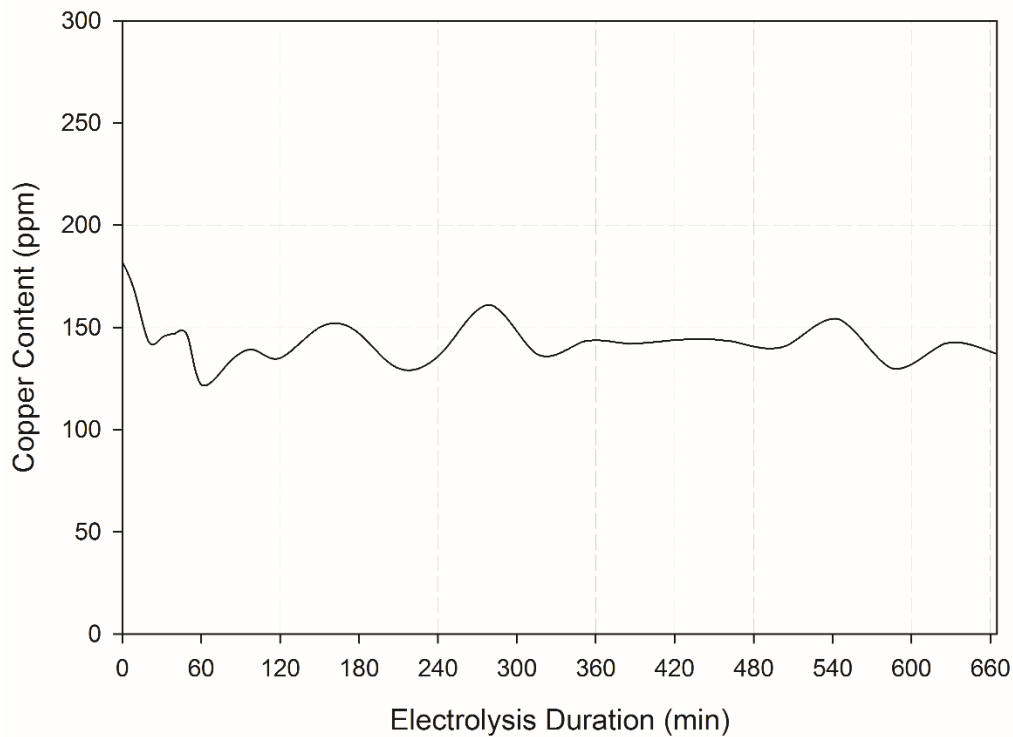


Figure 26. Borçelik pilot test at 100 A/m² pulse current density

After the operation at 100 A/m² average pulse current density, the study was repeated by using 130 A/m² average pulse current density. The amount of copper in the solution versus electrolysis time is given in Figure 27. The copper concentration of the solution was reduced from 159 ppm to 126 ppm. This indicates that the collected copper corresponds to about 21%. Although the result was less than that given in Figure 26, the effect of initial copper concentration should also be considered due to increased copper ion activity.

During this operation, approximately 865 liters of acid was passed through the line for 12 hours, indicating a speed of 1.2 L/min. The electrode area was designed to collect 25% copper when the flow rate is 1.0 L/min for the acid. If the result is proportioned to the flow rate of 1 L/min, the efficiency would become 25% which satisfies the expectation.

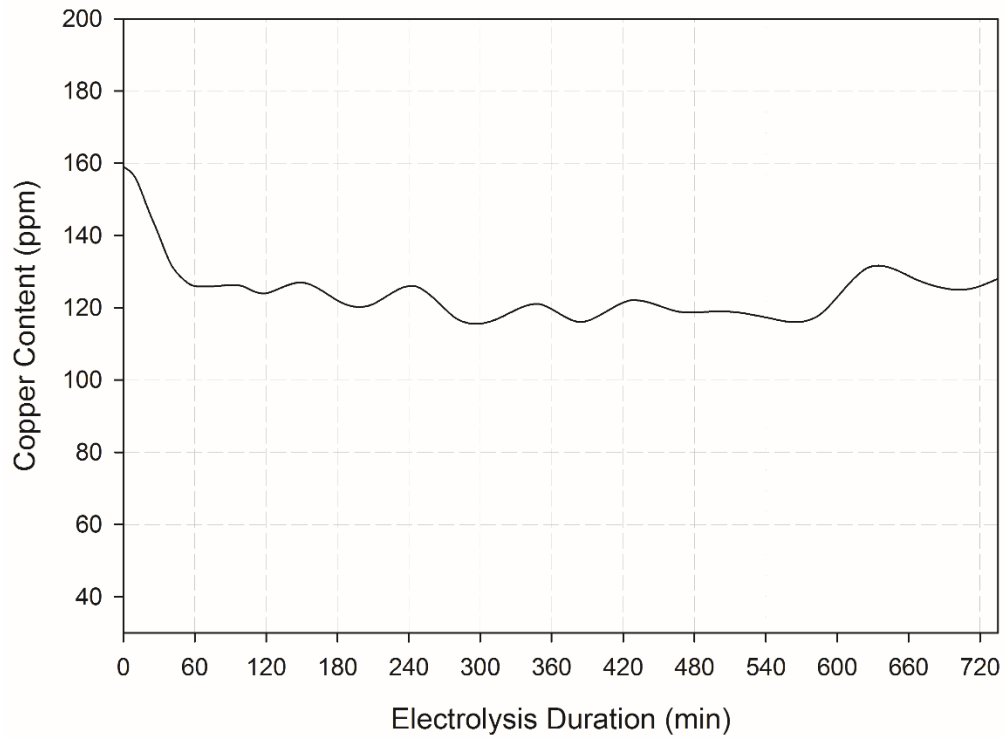


Figure 27. Borçelik pilot test at 130 A/m² pulse current density

In order to see that it is possible to decrease the copper level below 100 ppm when the initial copper concentration is around 125 ppm, the operation was repeated at 130 A/m² average pulse current density and 1 L/min flow rate with an initial copper concentration of 127 ppm. The amount of copper in the solution with respect to electrolysis time is given in Figure 28. The copper concentration was reduced from 127 to 80 ppm. This indicated 37% copper removal which meets the purpose of the study and in that way, copper deposition on the steel strip during pickling problem could be solved.

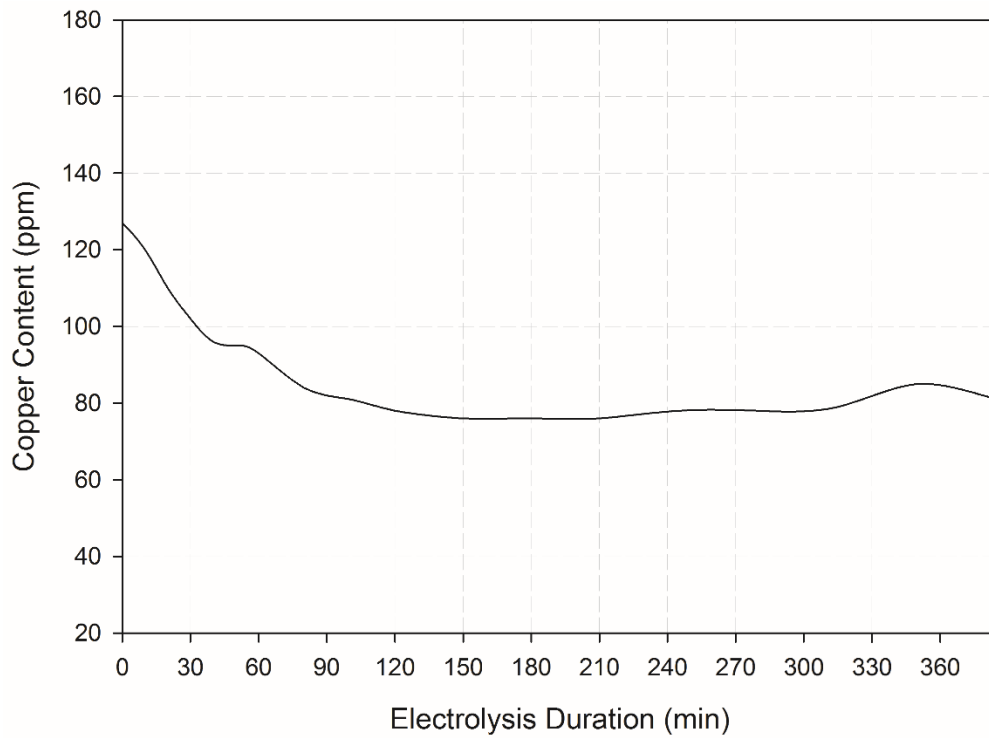


Figure 28. Borçelik pilot test result from 127 ppm initial copper concentration performed at 130 A/m^2 pulse current density

Figure 29 is the copper plated stainless steel cathode after the pilot test result of Figure 28. From the figure it can be seen that the corners were thicker than the surface due to the edge effect as it was expected from the COMSOL Multiphysics results.



Figure 29. Copper plated stainless steel cathode

In order to make the operation easier and converge to industrial application, it was decided to continue by direct current method. Direct current application on Borçelik Pilot Plant was performed at 150 A/m^2 current density. This current density was selected to yield identical copper removal efficiency with 130 A/m^2 pulse current density applications. The amount of copper in the solution as a function of electrolysis time is given in Figure 30. The reduction in copper concentration was 33 % and the final copper concentration was measured as 93 ppm. Therefore, it was concluded that direct current also satisfied the requirement.

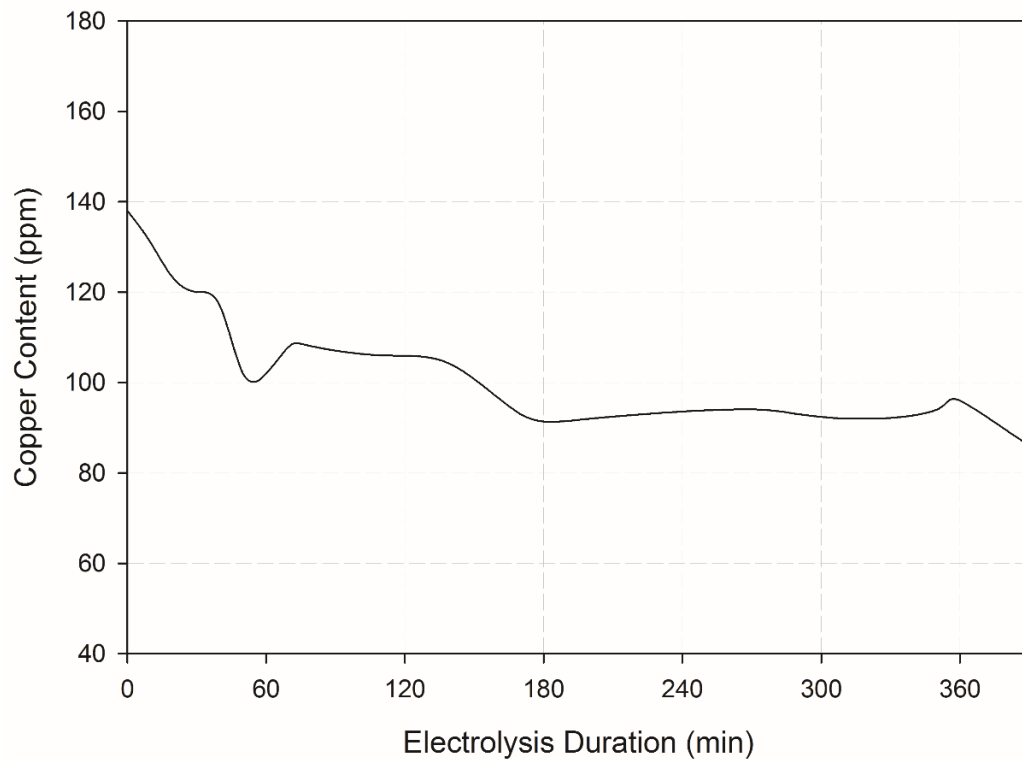


Figure 30. Borçelik pilot test at 150 A/m^2 direct current density

Finally, another experiment was conducted for 24 hours to measure the carrying capacity of the cathodes. Direct current application was performed on the system using 150 A/m^2 current density. The amount of copper in the solution with respect

to electrolysis time is given in Figure 31. ICP-MS analysis results were evaluated to determine the carrying capacity of the cathodes. It was expected to see a sudden increase in copper content from the ICP-MS results for the capacity determination. However, such a jump was only seen at the minute of 550 and the jump recovered in later measurements and was not encountered again. Results showed no significant change in copper dissolution. The copper concentration was reduced from 128 to 81 ppm. This corresponded to about 37% copper removal or copper collection. Therefore, carrying capacity of the cathodes was more than 24 hours.

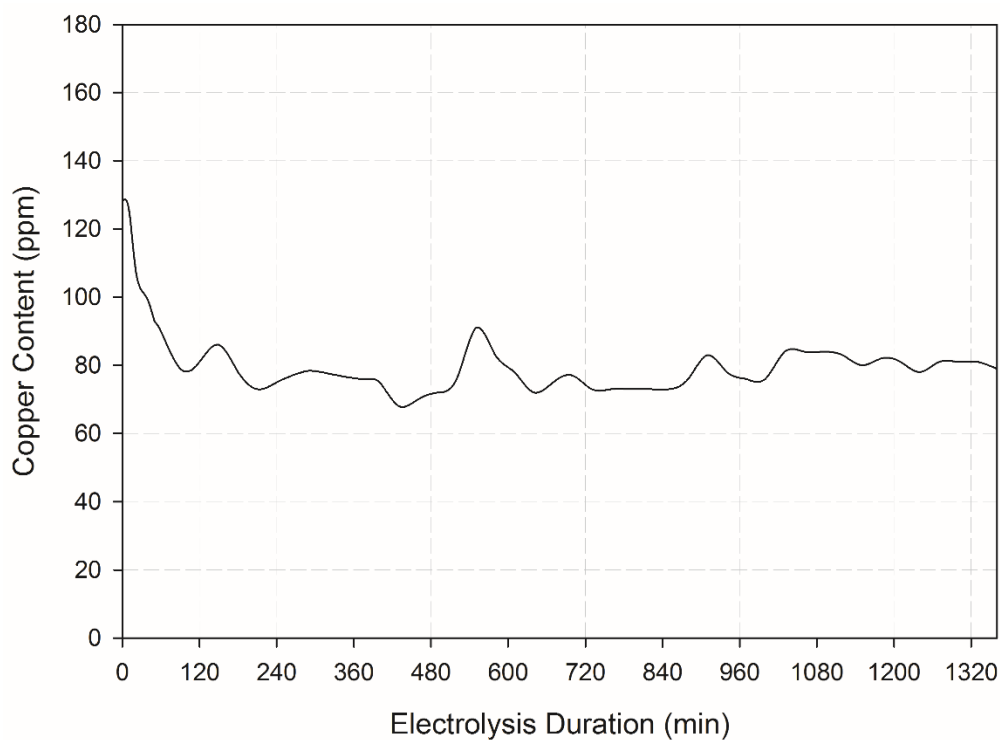


Figure 31. Borçelik pilot test for 24-hours of electrolysis at 150 A/m² direct current density

4.6 Evaluation of Acidity Change during Electrolysis

Electrolysis process was carried out to extend the lifetime of the pickling solution by removing trace amounts of copper from the solution. However, the process should not affect the properties of the acid adversely. During the laboratory and pilot tests, pH and conductivity of the solutions were measured before and after the process. There was not significant difference between two measurements of the pH and conductivity results. Furthermore, the acidity measurements revealed even an increase due to the anodic reaction of water electrolysis.

The change in conductivity of the acid for 24 hours electrolysis is shown in Figure 32.

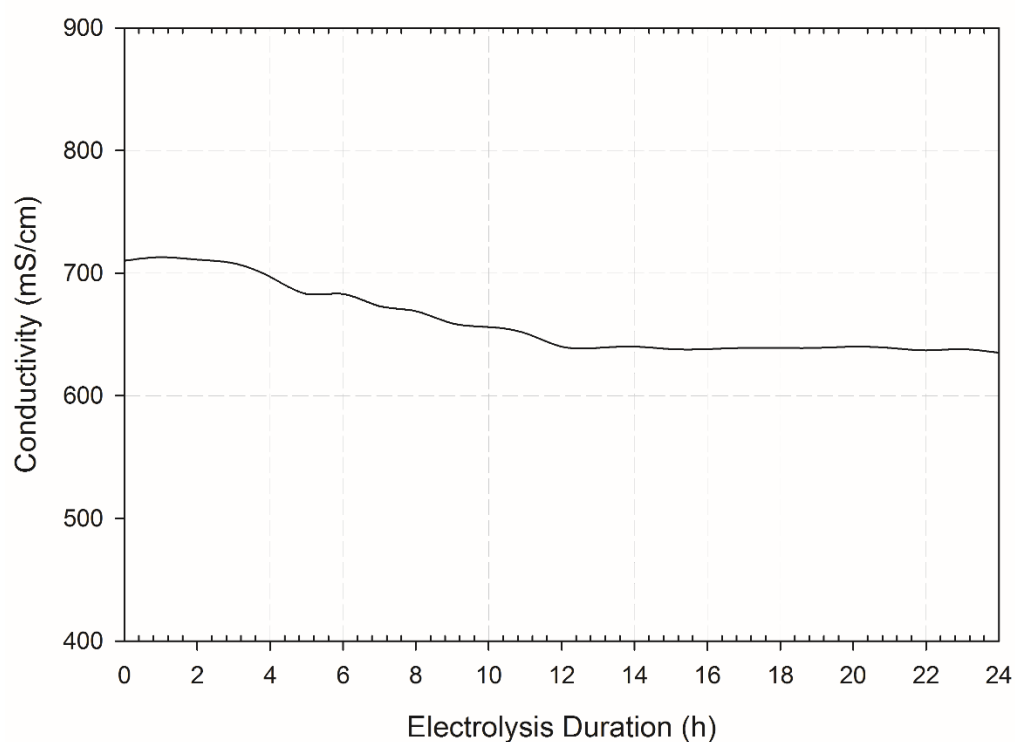


Figure 32. Change in conductivity with respect to electrolysis duration

4.7 Energy Consumption

In order to make the operation easier, it is decided to design the industrial process with direct current application. When the direct current studies were evaluated, the system can be operated at a current density of 150 A/m^2 . When considering Figure 31, the potential difference between anodes and cathodes was 7 V and the energy required to collect copper was calculated as approximately 102 kWh/kg of collected copper.

CHAPTER 5

CONCLUSION

An electrochemical batch reactor was developed to recover copper from the pickling solution of Borçelik steel plant. The spent pickling solution was composed of hydrochloric acid solution containing iron ions together with trace amounts copper and other ions. But the regenerated pickling solution contained trace amount of copper and iron ions. Copper removal from regenerated acid gave better results, therefore the studies were done with regenerated pickling solution of the steel plant.

A current density of 150 A/m^2 for direct current and an average current density of 130 A/m^2 for pulse current was selected to avoid too much H_2 evolution at the cathode, the possibility of Cl_2 evolution at the anode and irregular copper deposition.

Graphite was chosen as the anode material, because it provided the best stability in hot acidic solution. Copper and stainless steel were studied as cathode candidates and stainless steel was preferred because it has much more resistance to the hot acid and its vapor but the cathode must be protected from the acid vapor, regardless of its material. Furthermore, stainless steel had a better copper collecting efficiency. It was possible to peel off the collected copper easily from the stainless steel surface after the experiments.

It was found that copper removal increased with increasing the initial copper concentration, current density, and electrolysis duration. It was seen that there was no significant change in the properties of the acid as tracked by pH and conductivity measurements within the ranges of the parameters covered in this study. Furthermore, the acidity measurements revealed an increase due to the anodic reaction of water electrolysis.

The copper removal efficiency, current efficiency and the energy consumption were calculated as 36.7%, 3% and 102 kWh/kg, respectively.

REFERENCES

- [1] T. E. U. Graedel, “Recycling Rates of Metals - A Status Report,” 2011.
- [2] Outokumpu, “Handbook of Stainless Steel,” *Sandvikens Tryckeri*, pp. 1–89, 2013.
- [3] K. E. Daehn, A. Cabrera Serrenho, and J. M. Allwood, “How Will Copper Contamination Constrain Future Global Steel Recycling?,” *Environ. Sci. Technol.*, vol. 51, no. 11, pp. 6599–6606, 2017, doi: 10.1021/acs.est.7b00997.
- [4] T. N. Kenichi Nakajima, Osamu Takeda, Takahiro Miki, Kazuyo Matsubae, Shinichiro Nakamura, “Thermodynamic Analysis of Contamination by Alloying Elements in Aluminum Recycling,” *Environ. Sci. Technol.*, vol. 44, no. 14, pp. 5594–5600, 2010, doi: 10.1021/es9038769.
- [5] L. Savov, E. Volkova, and D. Janke, “Copper and Tin in Steel Scrap Recycling,” *Mater. Geoenvironment*, vol. 50, no. 3, pp. 627–640, 2003.
- [6] US Department of Commerce, “Steel Exports Report : Turkey,” pp. 1–8, 2016.
- [7] T. S. Producers, “Turkish Steel Industry,” *Turkish Steel Producers Association*, 2018. [Online]. Available: <http://celik.org.tr/en/english-turkish-steel-industry/>. [Accessed: 25-Oct-2019].
- [8] B. H. Anders Bornmyr, *Handbook for the Pickling and Surface Treatment of Stainless Steels*. 1995.
- [9] M. Bianchi, “Process for Stainless Steel Pickling and Passivation without Using Nitric Acid,” 1999.
- [10] A. Devi, A. Singhal, and R. Gupta, “A Review on Spent Pickling Liquor,” *Int. J. Environ. Sci.*, vol. 4, no. 3, pp. 284–295, 2013, doi: 10.6088/ijes.2013040300007.

- [11] P. V. Ghare NY, Wani KS, “A Review on Methods of Recovery of Acid(s) from Spent Pickle Liquor of Steel Industry,” *J. Environ. Sci. Eng.*, vol. 55, no. 2, pp. 253–266, 2013.
- [12] I. Noh and H. Park, “Acid Concentration Control for Pickling Line of Cold Rolling,” *IFAC-PapersOnLine*, vol. 48, no. 17, pp. 39–41, 2015, doi: 10.1016/j.ifacol.2015.10.074.
- [13] M. A. Nicholls, Z. Koont, B. D. Nelson, D. Bray, and J. Felker, “Copper Plating Phenomenon during the Pickling of Steel,” *Iron Steel Technol.*, vol. 5, no. 10, pp. 109–116, 2008.
- [14] Homer F. Staley, “The Theory of Pickling of Sheet Iron and Steel for Enameling Purposes,” *J. Am. Ceram. Soc.*, vol. 9, no. 12, pp. 787–796, 1926.
- [15] M. Tomaszewska, M. Gryta, and A. W. Morawski, “Recovery of Hydrochloric Acid from Metal Pickling Solutions by Membrane Distillation,” *Sep. Purif. Technol.*, vol. 22, no. 3, pp. 591–600, 2001, doi: 10.1016/S1383-5866(00)00164-7.
- [16] M. Rozenblat, M. Regel-rosocka, and J. Szymanowski, “Metal Removal From Spent Pickling Solutions of High Zinc(II) Concentration,” *Physicochem. Probl. Miner. Process.*, vol. 38, pp. 121–129, 2004.
- [17] F. Rögener, M. Sartor, A. Bán, D. Buchloh, and T. Reichardt, “Metal Recovery from Spent Stainless Steel Pickling Solutions,” *Resour. Conserv. Recycl.*, vol. 60, pp. 72–77, 2012, doi: 10.1016/j.resconrec.2011.11.010.
- [18] M. Regel-Rosocka, A. Cieszynska, and M. Wisniewski, “Methods of Regeneration of Spent Pickling Solutions from Steel Treatment Plants,” *Polish J. Chem. Technol.*, vol. 9, no. 2, pp. 42–45, 2007, doi: 10.2478/v10026-007-0023-x.
- [19] B. Tang, W. Su, J. Wang, F. Fu, G. Yu, and J. Zhang, “Minimizing the Creation of Spent Pickling Liquors in a Pickling Process with High-

- Concentration Hydrochloric Acid Solutions: Mechanism and Evaluation Method,” *J. Environ. Manage.*, vol. 98, pp. 147–154, 2012, doi: 10.1016/j.jenvman.2011.12.027.
- [20] M. K. Sinha, S. K. Sahu, P. Meshram, and B. D. Pandey, “Solvent Extraction and Separation of Zinc and Iron from Spent Pickle Liquor,” *Hydrometallurgy*, vol. 147–148, pp. 103–111, 2014, doi: 10.1016/j.hydromet.2014.05.006.
- [21] M.-S. L. Ton-Shyun Lin, Po-Jung Tseng, Jong-Kang Huang, “Treatment for Waste Pickling Solutions Containing Iron and Method of Ferroxide Formation,” 2004.
- [22] W. K. Karner and D. G. Gamsriegler, “Process for Regenerating Hydrochloric Acid from Pickling Plants,” 2001.
- [23] D. U. Ueberle, R. M. Michels, and H. W. Welling, “Process For Regenerating Used Hydrochloric Acid Containing Pickling Liquors,” US3399964, 1968.
- [24] R. Bjork, V. Tikate, H. L. Frandsen, and N. Pryds, “The Effect of Particle Size Distributions on the Microstructural Evolution during Sintering,” *J. Am. Ceram. Soc.*, vol. 96, no. 1, 2012, doi: 10.1111/jace.12100.
- [25] K. Yıldız, “Ellingham Diyagramları,” in *Metalürji Termodinamiği - 1*, pp. 82–87.
- [26] “The Characteristics of Copper, and the Reaction of the Metal with Nitric Acid,” *MEL Science*. [Online]. Available: <https://melscience.com/en/articles/characteristics-copper-and-reaction-metal-nitric-a/>. [Accessed: 10-Sep-2019].
- [27] N. Walker and D. L. George, “Oxidation of Copper by Hydrochloric Acid,” *J. Chem. Educ.*, vol. 45, no. 5, 1968, doi: 10.1021/ed045pA429.2.
- [28] “Methods of Copper Oxidation,” *MEL Science*. [Online]. Available: <https://melscience.com/en/articles/methods-copper-oxidation/>. [Accessed: 05-Nov-2019].

- [29] “Inductively Coupled Plasma Mass Spectrometry,” *TEAM Analytical Department*, p. 84, 2006.
- [30] L. T, “The History of Copper Cementation on Iron — The World’s First Hydrometallurgical Process from Medieval China,” *Hydrometallurgy*, vol. 17, no. 1, pp. 113–129, 1986.
- [31] M. El-Batouti, “Removal of Copper Metal by Cementation Using a Rotating Iron Cylinder,” *J. Colloid Interface Sci.*, vol. 283, no. 1, pp. 123–129, 2005, doi: 10.1016/j.jcis.2004.08.185.
- [32] G. D. Sulka and M. Jaskuła, “Influence of the Sulphuric Acid Concentration on the Kinetics and Mechanism of Silver Ion Cementation on Copper,” *Hydrometallurgy*, vol. 77, no. 1–2, pp. 131–137, 2005, doi: 10.1016/j.hydromet.2004.10.016.
- [33] H. Temur, A. Yartaşı, and M. M. Kocakerim, “A Study on the Optimum Conditions of the Cementation of Copper in Chlorination Solution of Chalcopyrite Concentrate by Iron Scraps,” *BAÜ Fen Bil. Enst. Derg.*, vol. 8, no. 2, pp. 63–73, 2006.
- [34] I. Yahiaoui and F. Aissani-Benissad, “Experimental Design for Copper Cementation Process in Fixed Bed Reactor Using Two-Level Factorial Design,” *Arab. J. Chem.*, vol. 3, no. 3, pp. 187–190, 2010, doi: 10.1016/j.arabjc.2010.04.009.
- [35] M. Hua, S. Zhang, B. Pan, W. Zhang, L. Lv, and Q. Zhang, “Heavy Metal Removal from Water/Wastewater by Nanosized Metal Oxides: A Review,” *J. Hazard. Mater.*, vol. 211–212, pp. 317–331, 2012, doi: 10.1016/j.jhazmat.2011.10.016.
- [36] “Copper,” *Royal Society of Chemistry*, 2017. [Online]. Available: <http://www.rsc.org/periodic-table/element/29/copper>. [Accessed: 25-May-2018].

- [37] M. T. Alvarez, C. Crespo, and B. Mattiasson, "Precipitation of Zn(II), Cu(II) and Pb(II) at Bench-Scale using Biogenic Hydrogen Sulfide from the Utilization of Volatile Fatty Acids," *Chemosphere*, vol. 66, no. 9, pp. 1677–1683, 2007, doi: 10.1016/j.chemosphere.2006.07.065.
- [38] P. Ghosh, A. N. Samanta, and S. Ray, "Reduction of COD and Removal of Zn²⁺ from Rayon Industry Wastewater by Combined Electro-Fenton Treatment and Chemical Precipitation," *Desalination*, vol. 266, no. 1–3, pp. 213–217, 2011, doi: 10.1016/j.desal.2010.08.029.
- [39] F. Fu, H. Zeng, Q. Cai, R. Qiu, J. Yu, and Y. Xiong, "Effective Removal of Coordinated Copper from Wastewater using a New Dithiocarbamate-Type Supramolecular Heavy Metal Precipitant," *Chemosphere*, vol. 69, no. 11, pp. 1783–1789, 2007, doi: 10.1016/j.chemosphere.2007.05.063.
- [40] Q. Chen, Z. Luo, C. Hills, G. Xue, and M. Tyrer, "Precipitation of Heavy Metals from Wastewater using Simulated Flue Gas: Sequent Additions of Fly Ash, Lime and Carbon Dioxide," *Water Res.*, vol. 43, no. 10, pp. 2605–2614, 2009, doi: 10.1016/j.watres.2009.03.007.
- [41] F. Fu and Q. Wang, "Removal of Heavy Metal Ions from Wastewaters: A Review," *J. Environ. Manage.*, vol. 92, no. 3, pp. 407–418, 2011, doi: 10.1016/j.jenvman.2010.11.011.
- [42] A. Dąbrowski, Z. Hubicki, P. Podkościelny, and E. Robens, "Selective Removal of the Heavy Metal Ions from Waters and Industrial Wastewaters by Ion-Exchange Method," *Chemosphere*, vol. 56, no. 2, pp. 91–106, 2004, doi: 10.1016/j.chemosphere.2004.03.006.
- [43] C. Ye, H. Yang, J. Lin, H. Zeng, and F. Yu, "Study on Ion Exchange Property of Removing Mn²⁺ and Fe²⁺ in Groundwater by Modified Zeolite," *Desalin. Water Treat.*, vol. 30, no. 1, pp. 114–121, 2012, doi: 10.5004/dwt.2011.1927.
- [44] J. Carrillo-Abad, M. García-Gabaldón, and V. Pérez-Herranz, "Study of the Zinc Recovery from Spent Pickling Baths by Means of an Electrochemical

- Membrane Reactor using a Cation-Exchange Membrane Under Galvanostatic Control,” *Sep. Purif. Technol.*, vol. 132, pp. 479–486, 2014, doi: 10.1016/j.seppur.2014.05.052.
- [45] F. Xie and D. B. Dreisinger, “Copper Solvent Extraction from Alkaline Cyanide Solution with Guanidine Extractant LIX 7950,” *Trans. Nonferrous Met. Soc. China (English Ed.)*, vol. 20, no. 6, pp. 1136–1140, 2010, doi: 10.1016/S1003-6326(09)60268-5.
- [46] P. Navarro and F. J. Alguacil, “Extraction of Copper from Sulphate Solutions by LIX 864 in Escaid 100,” *Miner. Eng.*, vol. 12, no. 3, pp. 323–327, 1999, doi: 10.1016/S0892-6875(99)00009-6.
- [47] E. A. Fouad, “Separation of Copper from Aqueous Sulfate Solutions by Mixtures of Cyanex 301 and LIX® 984N,” *J. Hazard. Mater.*, vol. 166, no. 2–3, pp. 720–727, 2009, doi: 10.1016/j.jhazmat.2008.11.114.
- [48] I. L. Dukov and S. Guy, “Solvent Extraction of Zinc(II) and Copper(II) with Mixtures of LIX 34 and Versatic 911 in Kerosene,” *Hydrometallurgy*, vol. 8, no. 1, pp. 77–82, Jan. 1982, doi: 10.1016/0304-386X(82)90032-9.
- [49] A. Molaei, O. Kökkılıç, and K. E. Waters, “An Investigation into Predispersed Solvent Extraction of Nickel (II) Ions from Dilute Aqueous Solutions,” *Sep. Purif. Technol.*, vol. 174, pp. 396–407, 2017, doi: 10.1016/j.seppur.2016.10.055.
- [50] G. W. Kentish, S.E.; Stevens, “Innovations in Separations Technology for the Recycling and Re-use of Liquid Waste Streams,” *Chem. Engeneering J.*, vol. 84, no. 2, pp. 149–159, 2001.
- [51] F. R. Valenzuela, C. Basualto, J. Sapag, and C. Tapia, “Pergamon Membrane Transport of Copper with LIX-860 from Acid Leach Waste Solutions,” *Miner. Eng.*, vol. 10, no. 12, pp. 1421–1427, 1997.
- [52] J. G. Dean, F. L. Bosqui, and K. H. Lanouette, “Removing Heavy Metals from

- Waste Water,” *Environ. Sci. Technol.*, vol. 6, no. 6, pp. 518–522, 1972, doi: 10.1021/es60065a006.
- [53] V. J. Inglezakis, M. A. Stylianou, D. Gkantzou, and M. D. Loizidou, “Removal of Pb(II) from Aqueous Solutions by using Clinoptilolite and Bentonite as Adsorbents,” *Desalination*, vol. 210, no. 1–3, pp. 248–256, Jun. 2007, doi: 10.1016/J.DESAL.2006.05.049.
- [54] S. Y. Huang, C. S. Fan, and C. H. Hou, “Electro-Enhanced Removal of Copper Ions from Aqueous Solutions by Capacitive Deionization,” *J. Hazard. Mater.*, vol. 278, pp. 8–15, 2014, doi: 10.1016/j.jhazmat.2014.05.074.
- [55] F. Sarfarazi and J. Ghoroghchian, “Electrochemical Copper Removal from Dilute Solutions by Packed Bed Electrodes,” *Microchem. J.*, vol. 50, no. 1, pp. 33–43, Aug. 1994, doi: 10.1006/MCHJ.1994.1055.
- [56] I. A. Khattab, M. F. Shaffei, N. A. Shaaban, H. S. Hussein, and S. S. Abd El-Rehim, “Electrochemical Removal of Copper Ions from Dilute Solutions using Packed Bed Electrode. Part I,” *Egypt. J. Pet.*, vol. 22, no. 1, pp. 199–203, 2013, doi: 10.1016/j.ejpe.2012.09.011.
- [57] S. Pulkka, M. Martikainen, A. Bhatnagar, and M. Sillanpää, “Electrochemical Methods for the Removal of Anionic Contaminants from Water - A Review,” *Sep. Purif. Technol.*, vol. 132, pp. 252–271, 2014, doi: 10.1016/j.seppur.2014.05.021.
- [58] G. Chen, “Electrochemical Technologies in Wastewater Treatment,” *Sep. Purif. Technol.*, vol. 38, no. 1, pp. 11–41, 2004, doi: 10.1016/j.seppur.2003.10.006.
- [59] W. Schwarzacher, “Electrodeposition: A Technology for the Future,” *Electrochem. Soc. Interface*, vol. 15, no. 1, pp. 32–33, 2006.
- [60] A.S. Pilla, M.M.E. Duarte, and C.E. Mayer, “Some Aspects of Removal of Copper and Cobalt from Mixed Ion Dilute Solutions,” *J. Appl. Electrochem.*,

vol. 30, pp. 831–838, 2000, doi: 10.1023/A:1003910830855.

- [61] T. H. Wani, “Electrochemical Cell, Its Working Principle, Setup and Representation,” *India Study Channel*, 2011.
- [62] D. Sobha Jayakrishnan, “Electrodeposition - The Versatile Technique for Nanomaterials,” in *Corrosion Protection and Control Using Nanomaterials*, Woodhead Publishing Limited, 2012, pp. 86–118.
- [63] M. Paunovic, M. Schlesinger, and D. D. Snyder, “Fundamental Considerations,” in *Modern Electroplating*, 2010, pp. 1–32.
- [64] A. Gomes, I. Pereira, B. Fernández, and R. Pereiro, “Electrodeposition of Metal Matrix Nanocomposites: Improvement of the Chemical Characterization Techniques,” 2011.
- [65] V. Torabinejad, M. Aliofkhazraei, S. Assareh, M. H. Allahyarzadeh, and A. S. Rouhaghdam, “Electrodeposition of Ni-Fe Alloys, Composites, and Nano Coatings—A Review,” *J. Alloys Compd.*, vol. 691, pp. 841–859, 2017, doi: 10.1016/j.jallcom.2016.08.329.
- [66] L. P. Bicelli, B. Bozzini, C. Mele, and L. D. Urzo, “A Review of Nanostructural Aspects of Metal Electrodeposition,” vol. 3, pp. 356–408, 2008.
- [67] L. I. Antropov, *Theoretical electrochemistry*. Mir Publications, 1977.
- [68] N. A. Gokcen and R. G. Reddy, “Reversible Galvanic Cells,” *Thermodynamics*, pp. 267–283, 1996, doi: 10.1007/978-1-4899-1373-9_14.
- [69] Y. Zhang, “Tin and Tin Alloys for Lead-Free Solder,” in *Modern Electroplating*, 2011, pp. 139–204.
- [70] A. J. Bard and L. R. Faulkner, *Electrochemical Methods - Fundamentals and Applications*. 1944.
- [71] T. O. M. Hasegawa, N. Yamachika, Y. Okinaka, Y. Shacham- Diamand,

- “Electrochemistry,” vol. 75, p. 349, 2007.
- [72] Paunovic, Milan Schlesinger, Mordechai and D. D. Schlesinger, “Fundamental Considerations,” in *Modern Electroplating*, 2010, p. 737.
- [73] D. R. Gabe, “The Role of Hydrogen in Metal Electrodeposition Processes,” *J. Appl. Electrochem.*, vol. 27, pp. 908–915, 1997, doi: 10.1016/S0920-5632(01)01598-5.
- [74] S. S. Djokic, *Modern Aspects of Electrochemistry*. 2010.
- [75] D. Nikoli and K. I. Popov, *Hydrogen Co-deposition Effects on the Structure of Electrodeposited Copper*. 2010.
- [76] K. Krishnaveni, T. S. N. Sankara Narayanan, and S. K. Seshadri, “Electrodeposited Ni-B-Si₃N₄ Composite Coating: Preparation and Evaluation of Its Characteristic Properties,” *J. Alloys Compd.*, vol. 466, no. 1–2, pp. 412–420, 2008, doi: 10.1016/j.jallcom.2007.11.104.
- [77] G. Orhan, G. Hapçı, and Ö. Keleş, “Application of Response Surface Methodology (RSM) to Evaluate the Influence of Deposition Parameters on the Electrolytic Cu-Zn Alloy Powder,” *Int. J. Electrochem. Sci.*, vol. 6, no. 9, pp. 3966–3981, 2011.
- [78] M. S. Chandrasekar and M. Pushpavanam, “Pulse and Pulse Reverse Plating- Conceptual, Advantages and Applications,” *Electrochim. Acta*, vol. 53, no. 8, pp. 3313–3322, 2008, doi: 10.1016/j.electacta.2007.11.054.
- [79] L. F. Senna and A. S. Luna, “Experimental Design and Response Surface Analysis as Available Tools for Statistical Modeling and Optimization of Electrodeposition Processes,” in *Electroplating*, 2012, pp. 147–166.
- [80] W. Lu, C. Ou, P. Huang, P. Yan, and B. Yan, “Effect of pH on the Structural Properties of Electrodeposited Nanocrystalline FeCo Films,” *Int. J. Electrochem. Sci.*, vol. 8, pp. 8218–8226, 2013.

- [81] J. W. Dini and D. D. Snyder, "Electrodeposition of Copper," in *Modern Electroplating*, 2010, pp. 33–78.
- [82] J. B. T. Jean L. Stojak, Jan Fransaer, *Review of Electrocodeposition*, vol. 7. 2001.
- [83] G. A. Di Bari, "Electrodeposition of Nickel," in *Modern Electroplating*, 2010, pp. 79–114.
- [84] H. Kockar, M. Alper, T. Sahin, and O. Karaagac, "Role of Electrolyte pH on Structural and Magnetic Properties of Co-Fe Films," *J. Magn. Magn. Mater.*, vol. 322, no. 9–12, pp. 1095–1097, 2010, doi: 10.1016/j.jmmm.2009.10.058.
- [85] W. Lu, P. Huang, C. He, and B. Yan, "XRD, SEM and XAS Studies of FeCo Films Electrodeposited at Different Current Density," *Int. J. Electrochem. Sci.*, vol. 8, no. 1, pp. 914–923, 2013.
- [86] M. Saitou, S. Oshiro, and S. M. Asadul Hossain, "Effect of Temperature on Nickel Electrodeposition from a Nickel Sulfamate Electrolyte," *J. Appl. Electrochem.*, vol. 38, no. 3, pp. 309–313, 2008, doi: 10.1007/s10800-007-9439-5.
- [87] A. Hovestad and L. J. J. Janssen, "Electrochemical Codeposition of Inert Particles in a Metallic Matrix," *J. Appl. Electrochem.*, vol. 25, pp. 519–527, 1995.
- [88] J. Fransaer, "Study of the Behaviour of Particles in the Vicinity of Electrodes," 1994.
- [89] H. B. T. W. Tomaszewski, L. C. Tomaszewski, "Composition of Finely Dispersed Particles with Metals," *Plating*, vol. 56, pp. 1234–1239, 1969.
- [90] F. K. Sautter, "Electrodeposition of Dispersion-Hardened Nickel-Al2O3 Alloys," vol. 110, no. 6, pp. 557–560, 1962.
- [91] A. Pelton, W. T. Thompson, C. Bale, and G. Eriksson, "F A C T

- Thermochemical Database for Calculations in Materials Chemistry at High Temperatures,” *High Temp. Sci.*, vol. 26, pp. 231–250, 1988.
- [92] E. J. F. Dickinson, H. Ekström, and E. Fontes, “COMSOL Multiphysics®: Finite Element Software for Electrochemical Analysis. A Mini-Review,” *Electrochem. commun.*, vol. 40, pp. 71–74, 2014, doi: 10.1016/j.elecom.2013.12.020.
- [93] COMSOL Inc., “Understand, Predict, and Optimize Engineering Designs with the COMSOL Multiphysics® Software,” 2018. .
- [94] Perkin Elmer, “Technical note: The 30-minute guide to ICP-MS,” *Perkin Elmer Sciex Instruments*, pp. 1–8, 2004.
- [95] “XRF Technology,” *Thermo Fisher Scientific*. [Online]. Available: <https://www.thermofisher.com/io/en/home/industrial/spectroscopy-elemental-isotope-analysis/spectroscopy-elemental-isotope-analysis-learning-center/elemental-analysis-information/xrf-technology.html>. [Accessed: 15-Oct-2019].
- [96] “X-Ray Fluorescence (XRF),” *Malvern Panalytical*. [Online]. Available: <https://www.malvernpanalytical.com/en/products/technology/x-ray-fluorescence>. [Accessed: 15-Oct-2019].
- [97] J. Carrillo-Abad, M. García-Gabaldón, E. Ortega, and V. Pérez-Herranz, “Influence of Zn²⁺ Ions on Copper Electrowinning from Sulfate Electrolytes,” *Sep. Purif. Technol.*, vol. 98, pp. 366–374, 2012.
- [98] G. Hodjaoglu and I. S. Ivanov, “Metal Recovery of Solid Metallurgical Wastes. Galvanostatic Electroextraction of Copper from Sulphate Electrolytes Containing Zn²⁺ and Fe²⁺ Ions,” *Bulg. Chem. Commun.*, vol. 46, no. 1, pp. 150–156, 2014.
- [99] D. W. Dew and C. V. Phillips, “The Effect of Fe(II) and Fe(III) on the Efficiency of Copper Electrowinning from Dilute Acid Cu(II) Sulphate

Solutions with the Chemelec Cell. Part II. The Efficiency of Copper Electrowinning from Dilute Liquors,” *Hydrometallurgy*, vol. 14, no. 3, pp. 351–367, 1985, doi: 10.1016/0304-386X(85)90044-1.

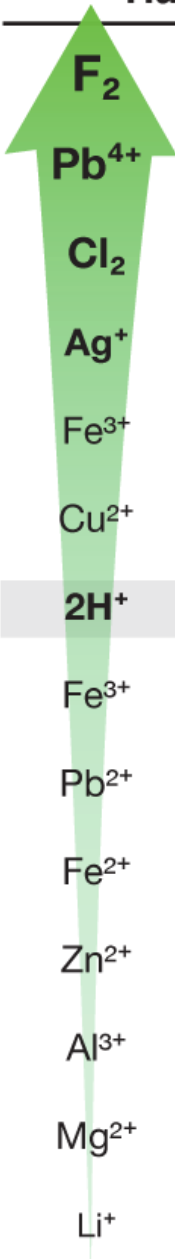
- [100] J. Carrillo-Abad, M. García-Gabaldón, E. Ortega, and V. Pérez-Herranz, “Recovery of Zinc from Spent Pickling Solutions using an Electrochemical Reactor in Presence and Absence of an Anion-Exchange Membrane: Galvanostatic Operation,” *Sep. Purif. Technol.*, vol. 98, pp. 366–374, Sep. 2012, doi: 10.1016/j.seppur.2012.08.006.
- [101] J. E. Oxley, “Electrolytic Regeneration of Acid Cupric Chloride Etchant,” 1995.
- [102] S. B. Wu Bin, “Process and System Device for Recovering Copper in Acid Etching Solution,” 2017.
- [103] “Electrolytic Dissociation of Metals from Sulphides,” 1974.
- [104] “Method of Producing Pure Nickel by Electrolytic Refining and Product Thus Obtained,” 1966.
- [105] J. R. Davis, *Surface Engineering for Corrosion and Wear Resistance*. 2001.
- [106] D. D. Snyder, “Preparation for Deposition,” in *Modern Electroplating*, 2010, pp. 507–512.
- [107] H. Han Verbung, “Copper Bath Composition for Electroless and/or Electrolytic Filling of Vias and Trenches for Integrated Circuit Fabrication,” 2004.
- [108] B. R. J. Beck Theodore R., “Electrolytic Reduction of Alumina,” 1991.
- [109] B. G. Hommeren and S. Kristiansand, “Electrolytic Refining of Nickel,” 1948.
- [110] “Introduction on MiniTab.” [Online]. Available: <https://www.greycampus.com/opencampus/minitab/introduction-on-minitab>.

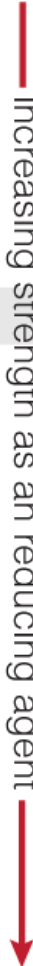
[Accessed: 06-Sep-2019].

- [111] “Minitab 19.” [Online]. Available: <http://www.minitab.com/en-us/products/minitab/>. [Accessed: 06-Sep-2019].
- [112] D. S. A. Bruce D. Craig, *Handbook of Corrosion Data*. ASM International, 1994.
- [113] I. M. Pohrelyuk O. I. Yas’kiv, “Corrosion of Titanium Alloys in Aqueous Solutions of Hydrochloric Acid,” *Mater. Sci.*, vol. 33, no. 3, pp. 375–378, 1997.
- [114] J. J. Bodner, “Dissolution of Titanium in Hydrochloric Acid,” University of Windsor, 1964.

APPENDICES

A. Standard Reduction Potential Table

	Half Reaction	potential
 increasing strength as an oxidizing agent	F₂ + 2e ⁻ ⇌ 2F ⁻	+2.87 V
	Pb⁴⁺ + 2e ⁻ ⇌ Pb ²⁺	+1.67 V
	Cl₂ + 2e ⁻ ⇌ 2Cl ⁻	+1.36 V
	Ag⁺ + 1e ⁻ ⇌ Ag	+0.80 V
	Fe³⁺ + 1e ⁻ ⇌ Fe ²⁺	+0.77 V
	Cu²⁺ + 2e ⁻ ⇌ Cu	+0.34 V
	2H⁺ + 2e⁻ ⇌ H₂	0.00 V
	Fe³⁺ + 3e ⁻ ⇌ Fe	-0.04 V
	Pb²⁺ + 2e ⁻ ⇌ Pb	-0.13 V
	Fe²⁺ + 2e ⁻ ⇌ Fe	-0.44 V
	Zn²⁺ + 2e ⁻ ⇌ Zn	-0.76 V
	Al³⁺ + 3e ⁻ ⇌ Al	-1.66 V
	Mg²⁺ + 2e ⁻ ⇌ Mg	-2.36 V
	Li⁺ + 1e ⁻ ⇌ Li	-3.05 V



 increasing strength as a reducing agent

B. List of Electronegativity Values of Elements

1	H	Hydrogen	2.2
2	He	Helium	no data
3	Li	Lithium	0.98
4	Be	Beryllium	1.57
5	B	Boron	2.04
6	C	Carbon	2.55
7	N	Nitrogen	3.04
8	O	Oxygen	3.44
9	F	Fluorine	3.98
10	Ne	Neon	no data
11	Na	Sodium	0.93
12	Mg	Magnesium	1.31
13	Al	Aluminum	1.61
14	Si	Silicon	1.9
15	P	Phosphorus	2.19
16	S	Sulfur	2.58
17	Cl	Chlorine	3.16
18	Ar	Argon	no data
19	K	Potassium	0.82
20	Ca	Calcium	1
21	Sc	Scandium	1.36
22	Ti	Titanium	1.54
23	V	Vanadium	1.63
24	Cr	Chromium	1.66
25	Mn	Manganese	1.55
26	Fe	Iron	1.83
27	Co	Cobalt	1.88
28	Ni	Nickel	1.91
29	Cu	Copper	1.9
30	Zn	Zinc	1.65
31	Ga	Gallium	1.81
32	Ge	Germanium	2.01
33	As	Arsenic	2.18
34	Se	Selenium	2.55
35	Br	Bromine	2.96
36	Kr	Krypton	3
37	Rb	Rubidium	0.82
38	Sr	Strontium	0.95
39	Y	Yttrium	1.22
40	Zr	Zirconium	1.33
41	Nb	Niobium	1.6
42	Mo	Molybdenum	2.16
43	Tc	Technetium	1.9
44	Ru	Ruthenium	2.2
45	Rh	Rhodium	2.28
46	Pd	Palladium	2.2
47	Ag	Silver	1.93
48	Cd	Cadmium	1.69
49	In	Indium	1.78
50	Sn	Tin	1.96
51	Sb	Antimony	2.05
52	Te	Tellurium	2.1
53	I	Iodine	2.66
54	Xe	Xenon	2.6
55	Cs	Cesium	0.79
56	Ba	Barium	0.89
57	La	Lanthanum	1.1
58	Ce	Cerium	1.12
59	Pr	Praseodymium	1.13
60	Nd	Neodymium	1.14
61	Pm	Promethium	1.13
62	Sm	Samarium	1.17
63	Eu	Europium	1.2
64	Gd	Gadolinium	1.2
65	Tb	Terbium	1.22
66	Dy	Dysprosium	1.23
67	Ho	Holmium	1.24
68	Er	Erbium	1.24
69	Tm	Thulium	1.25
70	Yb	Ytterbium	1.1
71	Lu	Lutetium	1.27
72	Hf	Hafnium	1.3
73	Ta	Tantalum	1.5
74	W	Tungsten	2.36
75	Re	Rhenium	1.9
76	Os	Osmium	2.2
77	Ir	Iridium	2.2
78	Pt	Platinum	2.28
79	Au	Gold	2.54
80	Hg	Mercury	2
81	Tl	Thallium	1.62
82	Pb	Lead	2.33
83	Bi	Bismuth	2.02
84	Po	Polonium	2
85	At	Astatine	2.2
86	Rn	Radon	no data
87	Fr	Francium	0.7
88	Ra	Radium	0.89
89	Ac	Actinium	1.1
90	Th	Thorium	1.3
91	Pa	Protactinium	1.5
92	U	Uranium	1.38
93	Np	Neptunium	1.36
94	Pu	Plutonium	1.28
95	Am	Americium	1.3
96	Cm	Curium	1.3
97	Bk	Berkelium	1.3
98	Cf	Californium	1.3
99	Es	Einsteinium	1.3
100	Fm	Fermium	1.3
101	Md	Mendelevium	1.3
102	No	Nobelium	1.3
103	Lr	Lawrencium	no data
104	Rf	Rutherfordium	no data
105	Db	Dubnium	no data
106	Sg	Seaborgium	no data
107	Bh	Bohrium	no data
108	Hs	Hassium	no data
109	Mt	Meitnerium	no data
110	Ds	Darmstadtium	no data
111	Rg	Roentgenium	no data
112	Cn	Copernicium	no data
113	Uut	Ununtrium	no data
114	Ff	Flerovium	no data
115	Uup	Ununpentium	no data
116	Lv	Livermorium	no data
117	Uus	Ununseptium	no data
118	Uuo	Ununoctium	no data

C. Analyzed Elements by ICP-MS

